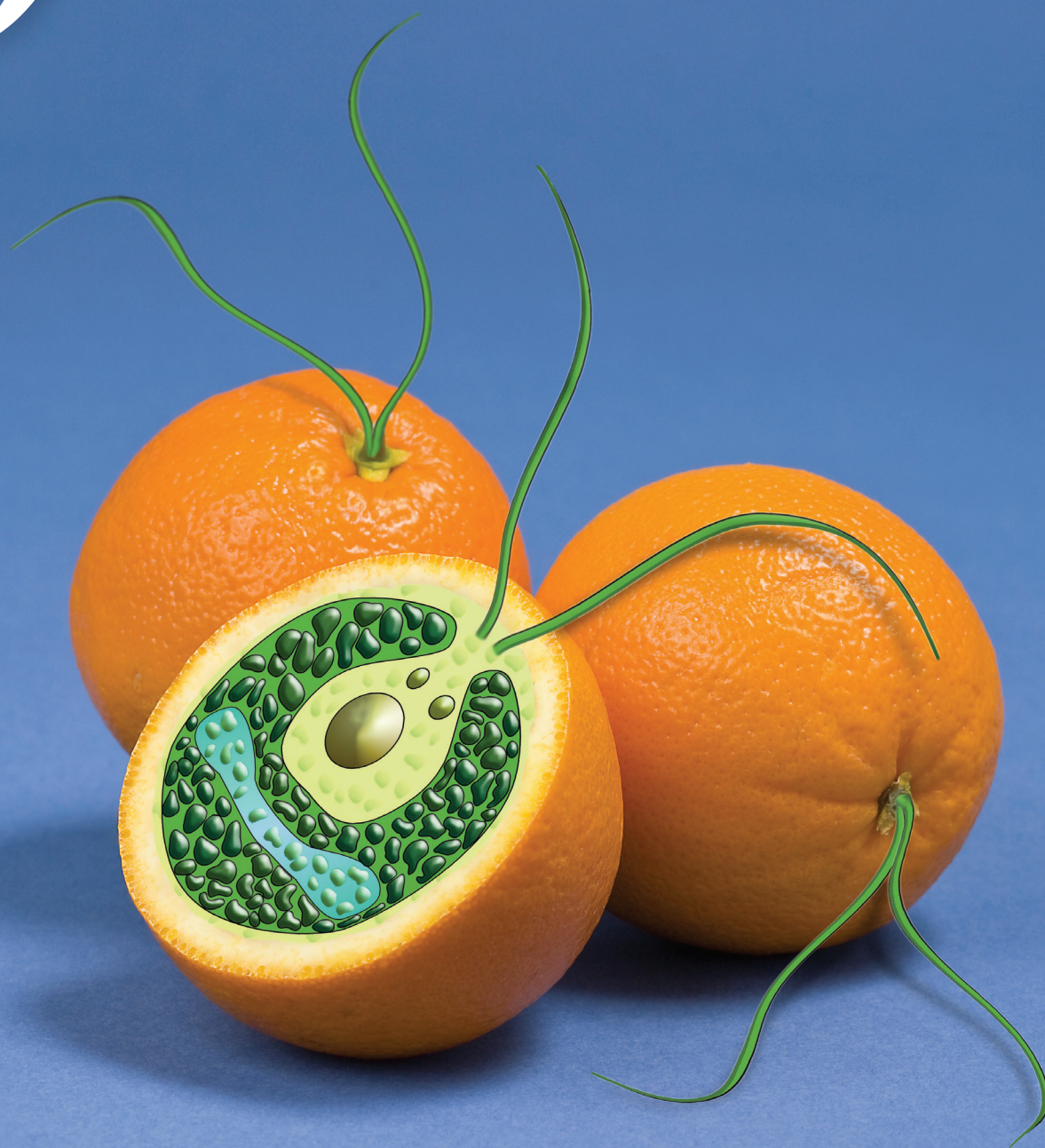


jbc the journal of biological chemistry

APRIL 20, 2012
VOLUME 287
NUMBER 17



AMERICAN SOCIETY FOR BIOCHEMISTRY AND MOLECULAR BIOLOGY

Impact of Oxidative Stress on Ascorbate Biosynthesis in *Chlamydomonas* via Regulation of the VTC2 Gene Encoding a GDP-L-galactose Phosphorylase^{*[5]}

Received for publication, January 11, 2012, and in revised form, February 23, 2012. Published, JBC Papers in Press, March 5, 2012, DOI 10.1074/jbc.M112.341982

Eugen I. Urzica[‡], Lital N. Adler[‡], M. Dudley Page[‡], Carole L. Linster^{‡§}, Mark A. Arbing[¶], David Casero^{||}, Matteo Pellegrini^{||}, Sabeeha S. Merchant^{‡¶**1}, and Steven G. Clarke^{‡***2}

From the Departments of [‡]Chemistry and Biochemistry, ^{||}Molecular, Cell, and Developmental Biology, and [¶]Institute of Genomics and Proteomics, ^{**}Molecular Biology Institute, UCLA, Los Angeles, California 90095 and the [§]de Duve Institute, Université Catholique de Louvain, BCHM 7539, Ave. Hippocrate 75, B-1200 Brussels, Belgium

Background: Ascorbate biosynthesis in plants occurs mainly via the L-galactose pathway.

Results: *Chlamydomonas reinhardtii* VTC2 encodes a GDP-L-galactose phosphorylase whose transcript levels are induced in response to oxidative stress concurrent with increased ascorbate accumulation.

Conclusion: Increased oxidative stress in *C. reinhardtii* results in an enzymatic and non-enzymatic antioxidant response.

Significance: First characterization of *C. reinhardtii* ascorbate biosynthesis and recycling pathways.

The L-galactose (Smirnoff-Wheeler) pathway represents the major route to L-ascorbic acid (vitamin C) biosynthesis in higher plants. *Arabidopsis thaliana* VTC2 and its paralogue VTC5 function as GDP-L-galactose phosphorylases converting GDP-L-galactose to L-galactose-1-P, thus catalyzing the first committed step in the biosynthesis of L-ascorbate. Here we report that the L-galactose pathway of ascorbate biosynthesis described in higher plants is conserved in green algae. The *Chlamydomonas reinhardtii* genome encodes all the enzymes required for vitamin C biosynthesis via the L-galactose pathway. We have characterized recombinant *C. reinhardtii* VTC2 as an active GDP-L-galactose phosphorylase. *C. reinhardtii* cells exposed to oxidative stress show increased VTC2 mRNA and L-ascorbate levels. Genes encoding enzymatic components of the ascorbate-glutathione system (e.g. ascorbate peroxidase, manganese superoxide dismutase, and dehydroascorbate reductase) are also up-regulated in response to increased oxidative stress. These results indicate that *C. reinhardtii* VTC2, like its plant homologs, is a highly regulated enzyme in ascorbate biosynthesis in green algae and that, together with the ascorbate recycling system, the L-galactose pathway represents the major route for providing protective levels of ascorbate in oxidatively stressed algal cells.

L-Ascorbic acid plays an essential role in plants by protecting cells against oxidative damage. In addition to its antioxidant role, L-ascorbic acid is also an important enzyme cofactor, for example, in violaxanthin de-epoxidase, required for dissipation of excess excitation energy, and prolyl hydroxylases (1–3). In plants, several pathways have been proposed to function in L-ascorbic acid biosynthesis. The best described pathway, the Smirnoff-Wheeler pathway or the L-galactose pathway, involves 10 enzymatic steps to convert D-glucose to L-ascorbic acid via intermediate formation of GDP-D-mannose, GDP-L-galactose, L-galactose-1-P, L-galactose, and L-galactono-1,4-lactone (4). Whereas the initial six steps are also involved in cell wall/glycoprotein biosynthesis, GDP-L-galactose phosphorylase (VTC2/VTC5) catalyzes the first committed step in L-ascorbic acid biosynthesis forming L-galactose-1-P (5, 6). L-Galactose-1-P phosphatase (VTC4),³ L-galactose dehydrogenase (L-Gal-DH), and L-galactono-1,4-lactone dehydrogenase (GLDH) catalyze the final steps in the Smirnoff-Wheeler pathway in higher plants such as *Arabidopsis thaliana* (7–9).

The biosynthesis of L-ascorbic acid is not characterized in detail in the green algae. Unicellular green algae such as the chlorophytes *Chlorella pyrenoidosa* and *Prototheca moriformis* can synthesize L-ascorbate using the L-galactose pathway (10–12). Two other photosynthetic unicellular protists (*Euglena gracilis* and *Ochromonas danica*) (13, 14) and a diatom (*Cyclotella cryptica*) utilize the inversion pathway commonly found in animals (supplemental Fig. S1) (15). Here we provide evidence that the Smirnoff-Wheeler pathway is completely conserved in the green alga *C. reinhardtii*. The VTC2 protein from *C. reinhardtii* is highly similar to higher plant VTC2/VTC5, containing the HXHXH motif characteristic of members of the HIT

* This work was supported, in whole or in part, by National Institutes of Health Grant GM026020 (to S. G. C.), the Division of Chemical Sciences, Geosciences and Biosciences, Office of Basic Energy Sciences of the United States Department of Energy Grant DE-FD02-04ER15529 (to S. S. M.), an Ellison Medical Foundation Senior Scholar Award (to S. G. C.), and UCLA Philip Whitcome and Graduate Division Dissertation Year Fellowships (to L. N. A.). The preparation of recombinant VTC2 enzyme was supported by the Department of Energy Grant DE-FC03-02ER63421 (to David Eisenberg).

[5] This article contains supplemental Figs. S1–S3 and Tables S1–S5. The nucleotide sequence(s) reported in this paper has been submitted to the GenBank™/EBI Data Bank with accession number(s) JQ246433.

¹ To whom correspondence may be addressed. E-mail: sabeeha@chem.ucla.edu.

² To whom correspondence may be addressed: Dept. Chemistry and Biochemistry, University of California, Los Angeles, 607 Charles E. Young Dr. E., Los Angeles, CA 90095. Tel.: 310-825-8300 or 310-825-8754; Fax: 310-206-1035 or 310-825-1968; E-mail: clarke@mbi.ucla.edu.

³ The abbreviations used are: VTC4, L-galactose-1-P phosphatase; L-Gal-DH, L-galactose dehydrogenase; GLDH, L-galactono-1,4-lactone dehydrogenase; APX, ascorbate peroxidase; MDAR, monodehydroascorbate reductase; DHAR, dehydroascorbate reductase; GSHR, glutathione reductase; MBP, maltose-binding protein; NDP, nucleoside diphosphate; HIT, histidine triad; tBuOOH, tert-butyl-hydroperoxide.

protein superfamily of nucleotide hydrolases and transferases (16).

Higher plants facing increased oxidative stress exhibit, in addition to increased *VTC2* mRNA and activity levels, elevated transcript abundance for all the enzymes of the vitamin C recycling pathway (ascorbate-glutathione system) in the chloroplast including ascorbate peroxidase (APX), monodehydroascorbate reductase (MDAR), dehydroascorbate reductase (DHAR), and glutathione reductase (GSHR) (2, 17). In this work, we found that *Chlamydomonas reinhardtii* cells facing oxidative stress have increased abundance of *VTC2* transcripts and all the enzymes of the ascorbate-glutathione system, as well as higher total ascorbate content. This suggests that *C. reinhardtii* cells respond to oxidative stress by producing more L-ascorbic acid both via *de novo* synthesis through the L-galactose pathway and via increased recycling.

EXPERIMENTAL PROCEDURES

Materials—ADP-D-Glc, GDP-D-Glc, GDP-D-Man, UDP-D-Gal, UDP-D-Glc (all in the α -configuration), GDP- β -L-Fuc, and GDP were from Sigma. GDP- β -L-Gal, synthesized and purified as described (18) was provided by Prof. Shinichi Kitamura (Osaka Prefecture University). This preparation was further purified by the reversed-phase HPLC method as described in Ref. 5. Fractions containing GDP-L-Gal were lyophilized, resuspended in H₂O, and stored at -20°C . Hydrogen peroxide (30%) and *tert*-butyl hydroperoxide (tBuOOH) (70%) were purchased from Fisher and Lancaster Synthesis, Inc., respectively. Ascorbate oxidase from *Cucurbita sp.* (EC 1.10.3.3; A0157) was purchased from Sigma.

Strains and Culture Conditions—*C. reinhardtii* strains 2137 (CC1021) and CC425 were obtained from the Chlamydomonas culture collection (Duke University) and grown in Tris acetate-phosphate (TAP) medium (19) at 24°C and $50\text{--}100\ \mu\text{mol m}^{-2}\ \text{s}^{-1}$ light intensity.

Sequencing of *C. reinhardtii* *VTC2*—The *VTC2* cDNA clone MXL096d05 (corresponding to EST BP098619) was completely sequenced. It contains the entire predicted *VTC2* open reading frame, 1857 bp long, encoding a protein of 618 amino acids. The open reading frame is flanked by 499 nt of 5' untranslated region and a 3' untranslated region of 1396 nt followed by a 68-nt poly(A) tail. The complete *VTC2* sequence has been deposited in NCBI (GenBank accession JQ246433).

***VTC2* Cloning**—The *VTC2* expression construct was generated by nested PCR and the Gateway recombinational cloning system (Invitrogen) as described (20). Briefly, the coding sequence of *VTC2* (amino acids D2-A618) was amplified with Phusion polymerase (New England Biolabs) from plasmid MXL096d05 using gene-specific primers with 5' extensions encoding a TEV protease cleavage site in the forward primer (*VTC2*.D2) and a C-terminal hexahistidine tag followed by a stop codon in the reverse primer (*VTC2*.A628) (supplemental Table S4). The initial product was then amplified with a second set of primers to introduce AttB1 and AttB2 recombination sites (PE-277 and PE-278) (supplemental Table S4). Amplification products were gel purified and recombined into the donor vector pDONR201 and subsequently into expression vector pKM596 (20) to produce an N-terminal His-tagged maltose-

binding protein (MBP) fusion using the Invitrogen protocol. DNA sequencing (Genewiz) was used to confirm the sequence of the expression construct.

***VTC2* Expression and Purification**—The expression plasmid was transformed into *Escherichia coli* BL21-Gold (DE3) cells (Novagen). Cells were grown in LB medium at 37°C to an $A_{600\ \text{nm}}$ of 0.6 at which point the temperature was shifted to 18°C and protein expression was induced by the addition of isopropyl 1-thio- β -D-galactopyranoside to a concentration of 1 mM. Cell growth was continued overnight and the cells were collected by centrifugation the following day. The cell pellet was resuspended in wash buffer (20 mM Tris, pH 8.0, 300 mM NaCl, 10 mM imidazole, 0.2% Nonidet P-40, 10% glycerol) supplemented with protease inhibitor mixture (Sigma), PMSF (100 μM), DNase (20 $\mu\text{g ml}^{-1}$), a few crystals of lysozyme, and 10 mM β -mercaptoethanol. Cells were lysed using a French press. The lysate was clarified by centrifugation (30 min at $35,000 \times g$) and the supernatant was incubated with nickel-nitrilotriacetic acid-agarose beads (Qiagen) for 60 min at 4°C . The beads were washed extensively with wash buffer and bound protein was eluted with elution buffer (wash buffer containing 300 mM imidazole). *VTC2* was further purified by size exclusion chromatography using a HiLoad Superdex S-200 column (GE Life Sciences) equilibrated in 20 mM Tris, pH 8.0, 300 mM NaCl, and 10% glycerol. Peak fractions were analyzed by SDS-PAGE and those containing *VTC2* were pooled and concentrated. Two peaks containing *VTC2* MBP fusion proteins were obtained by size exclusion chromatography. Both peaks contained pure MBP-*VTC2* fusion protein and were pooled separately and concentrated. The fraction showing the highest activity was used for enzymatic analyses.

Nucleic Acid Analysis—Total RNA was extracted from exponentially growing *C. reinhardtii* cells as previously described (21). RNA quality was assessed using an Agilent 2100 Bioanalyzer and RNA blot hybridization for *CBLP* as described (22). The probe used for detection was a 915-bp EcoRI fragment from the cDNA insert (encoding *CBLP*) in plasmid pcf8-13 (23).

Quantitative Real-time PCR on cDNA—cDNA synthesis and quantitative real-time PCR was performed on technical triplicates as described (22) using the gene-specific primers listed in supplemental Table S5. The data are presented as the fold-change in mRNA abundance, normalized to an endogenous reference transcript (*CBLP* or *UBQ2*), relative to the sample grown before 1 mM H₂O₂ or 0.1 mM tBuOOH treatment (time 0). The abundance of the two reference transcripts did not change under the conditions tested.

Ascorbate Measurements—*C. reinhardtii* cells were grown in TAP medium to a density of 3×10^6 cells ml⁻¹, collected by centrifugation at $2,500 \times g$ for 5 min, resuspended in extraction buffer containing 2% metaphosphoric acid, 2 mM EDTA, and 5 mM DTT and stored at -80°C . To prepare extracts for vitamin C analysis, cells were lysed by freeze/thaw cycling and the soluble fractions were separated by centrifugation ($16,100 \times g$, 10 min at 4°C). Vitamin C content was measured by reversed-phase HPLC on an Econosphere C-18 column (5 μm bead size, 4.6×250 mm; Alltech Associates, Deerfield, IL) using a Hewlett Packard Series II 1090 liquid chromatograph. A

Ascorbate Biosynthesis and Regulation in *Chlamydomonas*

mobile-phase gradient of 0–40% acetonitrile in 20 mM triethyl ammonium acetate, pH 6.0, was used at a flow rate of 1 ml min⁻¹. The injection volume was 50–100 μ l. Ascorbic acid was detected by monitoring the absorbance at 265 nm. The ascorbic acid peak was identified by comparison with the elution time of an L-ascorbate standard and by demonstrating a decrease of the peak area after the samples were treated with ascorbate oxidase. This treatment was performed by adding 2 units of ascorbate oxidase from *Cucurbita* sp. (EC 1.10.3.3) to 60 μ l of the extract in a final concentration 0.12 M monosodium citrate for 1 h at 4 °C. The final pH of the reaction was about 5.6. The differences in the peak areas measured before and after addition of ascorbate oxidase were used to calculate ascorbic acid levels based on a standard curve. The cellular concentration of L-ascorbate was determined using a cell volume of 140 femtoliters (24).

HPLC-based Nucleoside Diphosphate (NDP)-Hexose Phosphorylase Assay—NDP-hexose phosphorylase activities of recombinant VTC2 enzyme were assayed by measuring NDP formation after incubation with NDP-hexose in a reaction mixture at pH 7.5 containing 50 mM Tris-HCl, 5 mM sodium phosphate, 10 mM NaCl, and 1 mM DTT. Reactions (26 °C) were initiated by enzyme addition and stopped after 5–10 min by heating at 98 °C for 5 min. After removal of precipitated protein by centrifugation, supernatants were analyzed by anion-exchange HPLC as described in Ref. 5. NDP and NDP-hexose concentrations were calculated by comparing the integrated peak areas with those of standard NDP or NDP-hexose solutions. GraphPad Prism (La Jolla, CA) was used to calculate K_m and V_{max} values.

RNA-Seq—Total RNA samples prepared from *C. reinhardtii* strain 2137 grown photoheterotrophically in the presence of 1 mM H₂O₂ for 30 and 60 min were sequenced on a GAIIx platform. cDNA libraries were made using the protocol from Illumina and sequenced as single-end 76-mers. Raw and processed sequence files are available at the NCBI Gene Expression Omnibus (accession number GSE34826). Sequence reads were aligned using Bowtie (25) in single-end mode and with a maximum tolerance of 3 mismatches to the Au10.2 transcript sequences corresponding to the version 4 assembly of the *C. reinhardtii* genome. Expression estimates were obtained for each individual run in units of RPKMs (reads per kilobase of mappable transcript length per million mapped reads) (26), after normalization by the number of aligned reads and transcript mappable length (27). Technical replicates were averaged to obtain per-sample expression estimates. Final expression estimates and fold-changes were obtained for each biological replicate.

Sequence and Phylogenetic Analyses—To search for orthologs/homologs of *A. thaliana* members of the L-galactose pathway in green algae, two BLAST searches were performed. In the first, protein sequences of the *A. thaliana* proteins were used as queries to search against algal genomes databases. Sequences of putative homologs were retrieved and used for the second query by performing BLASTp against the *A. thaliana* database. If in the second query the highest-scoring homolog in *A. thaliana* was exactly the original *A. thaliana* query sequence, that protein was considered an ortholog (mutual best hit). Phylogenetic relationships were inferred using the Maximum Like-

lihood method based on the Whelan and Goldman model (28). The tree with the highest log likelihood is shown. Branch lengths reflect the number of substitutions per site. All positions containing gaps and missing data were eliminated. Alignment of putative VTC2 homologs was performed using MUSCLE, and evolutionary analyses were conducted in MEGA5 (29).

RESULTS

The *C. reinhardtii* Genome Encodes a Homolog of Plant GDP-L-galactose Phosphorylase—Biosynthesis of vitamin C in higher plants occurs mainly via the L-galactose pathway (9). In *A. thaliana*, the first committed step in the sequence of 10 enzymatic reactions from D-glucose to L-ascorbate is conversion of GDP-L-galactose to L-galactose-1-P, a reaction catalyzed by the GDP-L-galactose phosphorylase VTC2. Therefore, we were interested in finding homologs of VTC2 in *C. reinhardtii* and other green algae such as *Volvox carteri*, *Chlorella* sp. NC64A, *Coccomyxa* sp. C169, *Micromonas* sp. RCC299, and *Ostreococcus* RCC809. BLASTp searches identified a VTC2 homolog (Cre13.g588150) in *C. reinhardtii* (supplemental Fig. S2). Cre13.g588150 exhibits 46% amino acid sequence identity to *A. thaliana* VTC2. The *A. thaliana* genome encodes a VTC2 paralog, VTC5, which shows enzymatic properties similar to those of VTC2 (30, 31). The *C. reinhardtii* protein has 47% identity to VTC5 at the amino acid level. Because the *C. reinhardtii* genome encodes only a single protein highly similar to *A. thaliana* VTC2/VTC5, we termed this protein Cre13.g588150 VTC2. The amino acid sequence of the VTC2 protein from *C. reinhardtii* does not contain any transmembrane domains. Several subcellular localization prediction programs (ChloroP, TargetP, Psort, and PredSL) indicated that *C. reinhardtii* VTC2 does not possess obvious organellar targeting sequences, suggesting that, like the plant homologs, it is most likely a cytosolic protein. *C. reinhardtii* VTC2 contains a highly conserved histidine triad (HIT) motif (HXHXH, where X is a hydrophobic residue) (supplemental Fig. S2). *C. reinhardtii* VTC2 is more closely related to the *Volvox* VTC2 protein and among algal homologs it appears that the *Micromonas* sp. and *Ostreococcus* sp. proteins are more closely related to higher plant VTC2 proteins than to the animal VTC2 homologs (Fig. 1).

Enzymatic Components of L-Galactose Pathway to Vitamin C Biosynthesis Are Conserved in Green Algae—Because higher plant VTC2 has orthologs in *C. reinhardtii* and other green algae, we investigated whether the green algae encode the rest of the components of the Smirnoff-Wheeler pathway. BLASTp and tBLASTn searches identified orthologs (defined as mutual best BLAST hit) for almost all L-galactose pathway enzymes in six green algae (*C. reinhardtii*, *V. carteri*, *Chlorella* sp. NC64A, *Coccomyxa* sp. C169, *Micromonas* sp. RCC299, and *Ostreococcus lucimarinus*). Orthologs of *A. thaliana* phosphomannose isomerase (PMI1), phosphomannomutase (PMM), GDP-D-mannose 3',5"-epimerase (GME1), L-galactose-1-P phosphatase (VTC4), L-Gal-DH, and GLDH are present in all six species (Fig. 2 and supplemental Table S1). Interestingly, our sequence analysis identified orthologs of GDP-D-mannose pyrophosphorylase (VTC1) in *C. reinhardtii*, *V. carteri*, *Chlorella* sp. NC64A, and *Coccomyxa* sp. C169, but not in *Micromonas* sp.

Ascorbate Biosynthesis and Regulation in *Chlamydomonas*

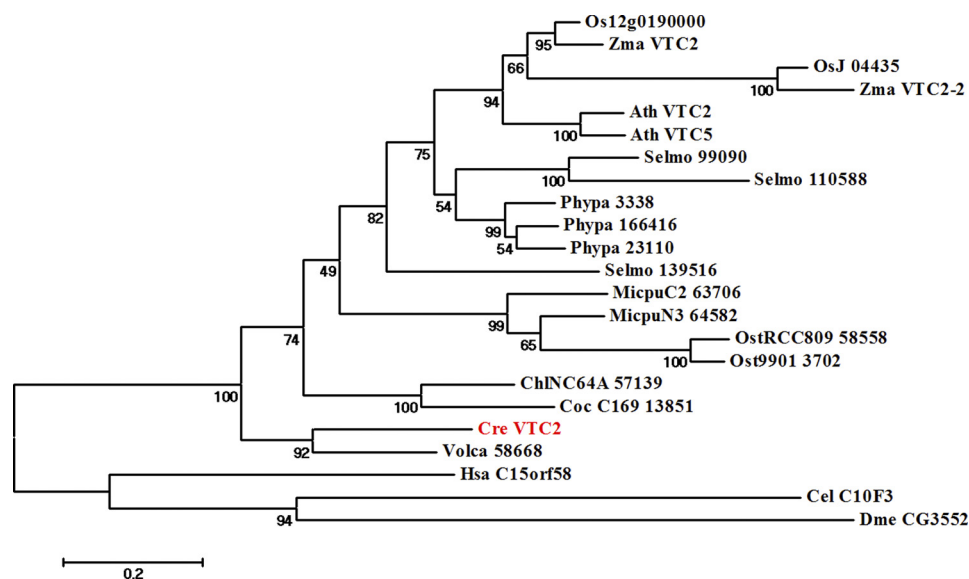


FIGURE 1. Phylogenetic tree of VTC2-like proteins. Protein sequences homologous to *C. reinhardtii* VTC2 were used to build the phylogenetic tree as described under "Experimental Procedures." Bootstrap values are shown below the branches. Bar, 0.2 amino acid substitutions per site. *C. reinhardtii* (Cre), *Coccomyxa* sp. C-169 (Coc_C169), *Chlorella* sp. NC64A (ChINC64A), *Volvox carterii* f. *nagariensis* (Vca), *O. lucimarinus* (Ost9901), *Ostreococcus* sp. RCC809 (OstRCC809), *M. pusilla* (MicpuC2), *Micromonas* sp. RCC299 (MicpuN3), *A. thaliana* (Ath), *Physcomitrella patens* (Ppa), *Ricinus communis* (Rco), *Oryza sativa* (Osa), *Selaginella moellendorffii* (Selmo), *D. melanogaster* (Dme), *C. elegans* (Cel), and *H. sapiens* (Hsa).

(RCC299 and *Micromonas pusilla*) nor in *Ostreococcus* sp. (*Ostreococcus tauri*, *Ostreococcus lucimarinus*, and *Ostreococcus* RCC899) (Fig. 2 and supplemental Table S1). *Micromonas* sp. and *Ostreococcus* sp. both belong to the class Prasinophyceae, which diverged at the base of the algal lineage and are therefore more distantly related to the chlorophyte algae. It is possible that *Micromonas* spp. and *Ostreococcus* spp. synthesize GDP-D-mannose using a different pathway (see "Discussion"). Overall, we conclude that the L-galactose pathway to L-ascorbate biosynthesis is conserved in the green algae.

Because alternative L-ascorbate biosynthetic pathways have been proposed (7, 32), we searched for orthologs/homologs of the enzymes catalyzing the proposed steps in these alternate pathways (supplemental Fig. S1). First, the proposed L-gulose pathway (33) involves the *A. thaliana* GDP-D-mannose 3",5"-epimerase, which is orthologous to *C. reinhardtii* SNE1. This enzyme can form GDP-L-gulose, which, if converted to L-gulonono-1,4-lactone, would provide a substrate for an oxidase reaction leading directly to L-ascorbate. Although *C. reinhardtii* GLDH demonstrates 30% amino acid sequence identity to the rat L-gulonono-1,4-lactone dehydrogenase/oxidase (Gulo) (34), and two other similar proteins are present (Cre14.g611650 with 26% amino acid identity and Cre03.g177600 with 22% amino acid identity), these putative enzymes have not been characterized and no homologs of enzymes converting GDP-L-gulose to L-gulonono-1,4-lactone have been found.

L-Gulonono-1,4-lactone could also be potentially formed from myo-inositol via D-glucuronate (supplemental Fig. S1, animal-like pathway). *C. reinhardtii* codes for a potential myo-inositol oxidase (Cre01.g025850) that might be responsible for the formation of D-glucuronate and shows 31% amino acid identity to *A. thaliana* MIOX4 (supplemental Table S1). Conversion of D-glucuronate to L-gulonate would require the action of a glucuronate reductase, which has not been identified in plants. Formation of L-gulonono-1,4-lactone from L-gulonate requires an

aldonolactonase (gulonolactonase) (35). SMP30 (senescence marker protein 30) has been recently identified to function as a glucono/gulonolactonase (36). The *C. reinhardtii* genome does not encode a homolog to SMP30. Hence, it seems unlikely that *C. reinhardtii* would use this route as an alternate pathway to vitamin C biosynthesis.

It has also been proposed that biosynthesis of L-ascorbic acid could occur via the galacturonate or salvage pathway (7, 9) (supplemental Fig. S1). This pathway would involve conversion of methyl-D-galacturonate to D-galacturonate. The enzyme catalyzing this reaction has not yet been identified. Formation of L-galactonate from D-galacturonate is catalyzed in ripening strawberry fruits by an aldo-keto reductase specific for D-galacturonate (GalUR) (37). The *C. reinhardtii* genome encodes several aldo-keto reductases with homology to strawberry D-galacturonate reductase (supplemental Table S1), but none of them is an ortholog of the plant enzyme. On the other hand, orthologs of the strawberry GalUR are present in other algal species such as *Chlorella* sp. NC64A, *Micromonas* sp. RCC299, *O. lucimarinus*, or *V. carteri* (supplemental Table S1). The penultimate reaction in the galacturonate pathway (L-galactonate to L-galactono-1,4-lactone conversion) would require the function of an aldonolactonase, which has been recently characterized in the protist *E. gracilis* (38). BLASTp and tBLASTn searches did not identify any homologs to *E. gracilis* aldonolactonase in *C. reinhardtii* or *V. carteri*, but orthologs are present in *Chlorella* sp. NC64A, *Coccomyxa* sp. C169, *Micromonas* sp. RCC299, and *O. lucimarinus* (supplemental Table S1).

We conclude that essential components of the alternate pathways to L-ascorbate biosynthesis are missing in *C. reinhardtii*. We could identify homologs of L-gulonono-1,4-lactone dehydrogenase for the L-gulose pathway and galacturonate reductase for the salvage pathway, but there are no orthologs to rat Gulo or strawberry GalUR and the sequence similarity is poor. On the other hand, we show that all components of the

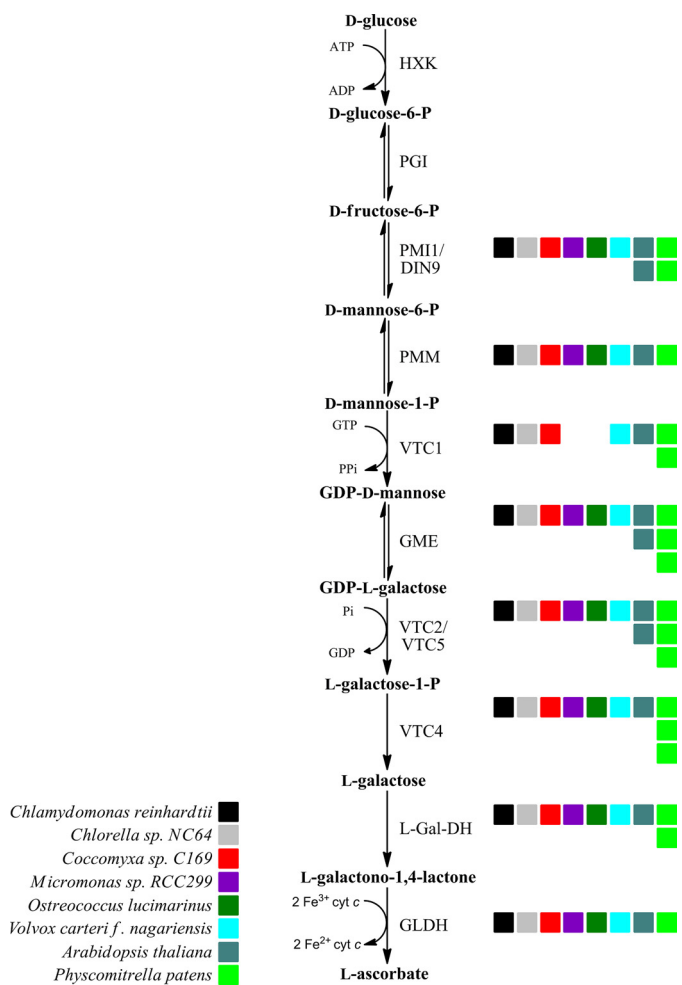


FIGURE 2. The L-galactose pathway of ascorbic acid biosynthesis is conserved in green algae. Colored squares indicate the number of *A. thaliana* orthologs present in each organism. The enzymes catalyzing the successive steps are hexokinase (HXK), phosphoglucose isomerase (PGI), phosphomannose isomerase (PIM), phosphomannomutase (PMM), GDP-L-mannose pyrophosphorylase (VTC1), GDP-D-mannose-3',5'-epimerase (GME), GDP-L-galactose phosphorylase (VTC2), L-galactose-1-P phosphatase (VTC4), L-Gal-DH, and GLDH.

plant Smirnoff-Wheeler pathway have orthologs in *C. reinhardtii* and in other algal species. These results point to a conserved L-galactose pathway to L-ascorbate biosynthesis, which might represent the major route to L-ascorbate biosynthesis in algae, in particular *C. reinhardtii* and other Volvocales.

Recombinant *C. reinhardtii* VTC2 Is a GDP-L-galactose/GDP-D-glucose Phosphorylase—Previous studies demonstrated that *A. thaliana* VTC2 and VTC5 are GDP-L-galactose phosphorylases, converting GDP-L-galactose into L-galactose-1-P and GDP in the presence of P_i (5, 30, 31). To test whether *C. reinhardtii* VTC2 can catalyze this reaction, recombinant *C. reinhardtii* VTC2 was purified as a His- and MBP-tagged protein. Because *A. thaliana* VTC2 shows GDP-L-galactose and GDP-D-glucose phosphorylase activities, we first determined the activity of the *C. reinhardtii* enzyme on various sugar nucleotides in the presence of inorganic phosphate (Table 1). Similar activity was seen with GDP-L-Gal and GDP-D-Glc, whereas a 2-fold lower activity was found with GDP-L-Fuc. No significant phosphorylase activity was measured with GDP-D-Man, UDP-

TABLE 1

Substrate specificity of recombinant *C. reinhardtii* VTC2

Various sugar nucleotides (50 μM) were incubated in the presence of *C. reinhardtii* VTC2 recombinant enzyme (0.025 $\mu\text{g ml}^{-1}$) for 10 min at 26 °C. With GDP-L-Gal as a substrate, the specific activity of the *C. reinhardtii* VTC2 enzyme was $25.4 \pm 5.1 \mu\text{mol min}^{-1} \text{mg protein}^{-1}$ (mean \pm S.D., $n = 3$); this value was taken as 100%. The phosphorylase activities found with the other sugar nucleotides are given as a percentage of the activity found with GDP-L-Gal \pm S.D. Values represent the means of 2–3 individual experiments for each substrate.

Substrate	Relative activity of recombinant <i>C. reinhardtii</i> VTC2
	% \pm S.D.
GDP-L-Gal	100
GDP-D-Glc	87.4 ± 29.2
GDP-L-Fuc	51.4 ± 15.1
GDP-D-Man	0 ± 0
UDP-D-Glc	0.5 ± 0.8
UDP-D-Gal	2.5 ± 4.1
ADP-D-Glc	3.7 ± 5.8

D-Glc, UDP-D-Gal, and ADP-D-Glc (Table 1). Thus, our data indicate that *C. reinhardtii* VTC2 possesses a similar nucleotide sugar substrate specificity as *A. thaliana* VTC2.

The conserved HIT motif (HXHXH) in *C. reinhardtii* VTC2 is typical of HIT hydrolases, whereas plant VTC2 proteins contain a HIT motif typical for HIT transferases/phosphorylases (HXHXQ) (16). Therefore, we tested the acceptor specificity of *C. reinhardtii* VTC2 by measuring the GDP-L-Gal or GDP-D-Glc consumption after incubation of the recombinant VTC2 enzyme with different possible acceptors. When recombinant *C. reinhardtii* VTC2 was incubated in the absence of P_i , we detected no hydrolytic activity (Fig. 3). However, in the presence of P_i , we observed a dramatic increase in GDP-L-Gal and GDP-D-Glc consumption (Fig. 3). Incubation of the enzyme with pyrophosphate (PP_i), D-Glc-1-P (in the presence of GDP-L-Gal), or L-Gal-1-P (in the presence of GDP-D-Glc) did not result in any significant nucleotide sugar substrate consumption (Fig. 3). Additionally, we did not detect the formation of GMP or GTP, the expected products of hydrolase or pyrophosphorylase activity, under any of these conditions (data not shown). These data clearly indicate that *C. reinhardtii* VTC2 is a phosphorylase like the *Arabidopsis* enzyme.

C. reinhardtii VTC2 has similar, low micromolar, Michaelis constants for both GDP-L-Gal and GDP-D-Glc (Table 2). Interestingly, with *C. reinhardtii* VTC2 we have found at least 10 times higher k_{cat} values for both substrates compared with the *A. thaliana* VTC2 recombinant enzyme, leading to about 10 times higher catalytic efficiencies for the former than for the latter enzyme (Table 2).

VTC2 Transcript Levels and Ascorbate Levels Are Increased in Response to Oxidative Stress—Previous studies have indicated that *A. thaliana* VTC2 mRNA levels are increased in leaves subjected to high light (30) and in seedlings grown in light compared with those grown in the dark (39). Therefore, we tested whether transcript levels of *C. reinhardtii* VTC2 respond to oxidative stress. *C. reinhardtii* was grown photoheterotrophically to $2 \times 10^6 \text{ cells ml}^{-1}$, then challenged with 1 mM H_2O_2 or 0.1 and 0.2 mM tBuOOH for 30, 60, 120, and 240 min. Both H_2O_2 and tBuOOH (an organic peroxide capable of inducing lipid peroxidation) treatments enhance intracellular reactive oxygen species production. The concentrations of H_2O_2 and tBuOOH and time points used in this study were

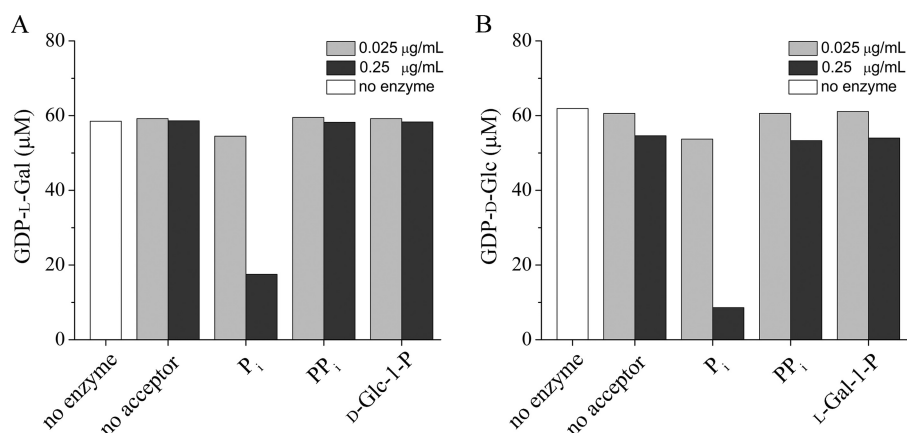


FIGURE 3. **Acceptor specificity of *C. reinhardtii* recombinant VTC2.** GDP-L-Gal and GDP-D-Glc consumption was measured by the HPLC assay described under "Experimental Procedures." GDP-L-Gal or GDP-D-Glc were added to the reaction mixtures at a final concentration of 50 μM . The consumption of GDP-L-Gal (A) and GDP-D-Glc (B) was measured with a final enzyme concentration of 0.025 $\mu\text{g/ml}$ (light gray bars) or 0.25 $\mu\text{g/ml}$ (dark gray bars).

TABLE 2

Characterization of the GDP-hexose phosphorylase activities of the recombinant *A. thaliana* and *C. reinhardtii* proteins

Values for the *A. thaliana* enzyme were taken from Linster *et al.* (5). K_m and V_{max} values for the *C. reinhardtii* VTC2 homolog were obtained by fitting the initial rate data to the Michaelis-Menten equation using the GraphPad Prism program. Enzymatic turnover numbers were derived from the V_{max} values by using a molecular mass of 110 kDa for His-MBP-tagged *C. reinhardtii* enzyme with the assumption that the enzyme preparations were pure. Incubation times and enzyme concentrations were adjusted to obtain initial velocity data. Enzymatic activities were measured by the HPLC assay as described under "Experimental Procedures." Values are the mean \pm S.D. calculated from 2–3 individual experiments for each substrate.

Substrate	k_{cat}		K_m		k_{cat}/K_m	
	<i>C. reinhardtii</i>	<i>A. thaliana</i>	<i>C. reinhardtii</i>	<i>A. thaliana</i>	<i>C. reinhardtii</i>	<i>A. thaliana</i>
GDP-L-galactose	615 \pm 3	64 \pm 8	0.008 \pm 0.001	0.010 \pm 0.001	9.2 \pm 1.3 $\times 10^7$	6.3 \pm 0.9 $\times 10^6$
GDP-D-glucose	813 \pm 277	23 \pm 3	0.0088 \pm 0.0029	0.0044 \pm 0.0016	8.0 \pm 1.3 $\times 10^7$	5.7 \pm 2.3 $\times 10^6$

previously shown to have no effect on cell growth in *C. reinhardtii* and yet were high enough to induce the antioxidant defense mechanisms (40–43). A lower concentration of tBuOOH was used because it was more stable than H_2O_2 under our culture conditions (supplemental Fig. S3). *VTC2* transcript abundance was assessed by real-time PCR. We found that *VTC2* mRNA transcript abundance increased 4-fold after 30 min and reached a maximum of 7-fold induction after 120 min exposure to 1 mM H_2O_2 (Fig. 4A). When *C. reinhardtii* cells were exposed to 0.1 mM tBuOOH, we observed a more dramatic induction in the *VTC2* transcript levels (50-fold increase after 30 min with the highest induction of 155-fold after 240 min). Increasing the tBuOOH concentration to 0.2 mM resulted in an even higher increase in the *VTC2* mRNA abundance (150-fold after 30 min and 250-fold after 120 min) (Fig. 4A).

To assess the overall impact of peroxide stress on the Smirnov-Wheeler pathway, we quantified the abundance of transcripts for each gene in the pathway in H_2O_2 -treated *versus* untreated cells. Changes in the *VTC2* transcript levels after H_2O_2 exposure observed by RNA-Seq are very similar to those observed by real-time PCR (6.4-fold induction after 30 min and 8.6-fold induction after 60 min) (Fig. 4B). Other components of the pathway including *MPII*, *PMM*, and *GMP1* showed at best a 2-fold increase in their transcript abundance after 60 min of exposure to H_2O_2 . The transcript levels of *SNE1*, *VTC4*, *L-GALDH*, and *GLDH* did not change significantly (Fig. 4B and supplemental Table S2) in response to H_2O_2 treatment. Together, the combined real-time PCR and RNA-Seq analyses demonstrated that *VTC2* mRNA levels are highly and selectively induced by oxidative stress, indicating that the GDP-L-galactose

phosphorylase step is potentially the key regulatory point of the L-ascorbate biosynthetic pathway in *C. reinhardtii*.

Next, we asked the question whether the increased *VTC2* mRNA levels correlate with a change in ascorbate content. Total ascorbate levels were measured in cell extracts from *C. reinhardtii* grown under 1 mM H_2O_2 or 0.1 mM tBuOOH stress for 2, 4, 6, and 8 h. Total ascorbate content increased progressively after addition of H_2O_2 , showing a slight increase after 2 h and reaching a maximum after 8 h, where we measured 7-fold higher ascorbate concentrations than in untreated cells (Fig. 5A). On the other hand, cells treated with 0.1 mM tBuOOH displayed a 4-fold higher ascorbate content 2 h after addition of tBuOOH, with a further increase after 4 h (5-fold). In contrast to *C. reinhardtii* cells exposed to H_2O_2 , after 6 h of tBuOOH treatment we noticed a drop in the total ascorbate levels (3-fold more compared with untreated cells), which decreased even further after 8 h to levels similar to those observed for untreated cells (Fig. 5B). The observation that tBuOOH treatment depletes cellular ascorbate has been made previously in rat hepatocytes (44) and rat astrocytes (45). Altogether, our results indicate a correlation between the *VTC2* mRNA levels and L-ascorbic acid content in *C. reinhardtii* cells exposed to oxidative stress.

Genes Encoding Components of Ascorbate-glutathione Scavenging System Are Induced in Response to Oxidative Stress—The ascorbate-glutathione cycle is a well known mechanism to scavenge H_2O_2 in various cell compartments (2), particularly in plants (46) (and see Fig. 7). Therefore, we were interested in expression profiles of the genes encoding the ascorbate-glutathione system components in *C. reinhardtii* cells exposed to 1

Ascorbate Biosynthesis and Regulation in *Chlamydomonas*

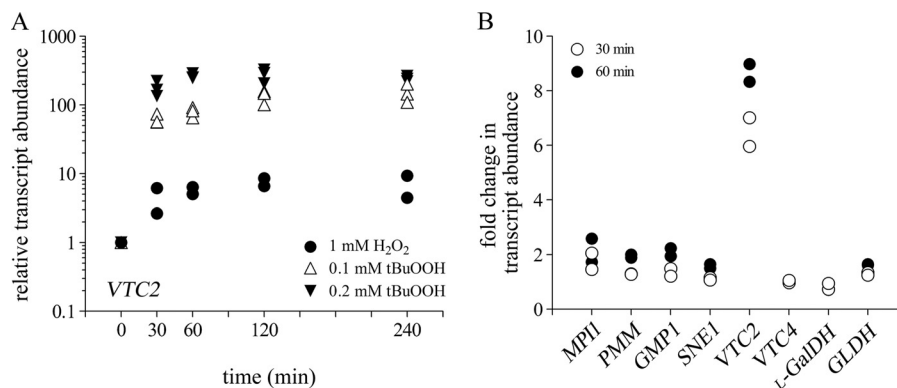


FIGURE 4. *VTC2* transcript levels are increased in response to oxidative stress. *A*, fold-change (\log_{10}) of *VTC2* transcript assessed by real-time PCR in *C. reinhardtii* cells grown photoheterotrophically in the presence of 1 mM H_2O_2 (filled circles), 0.1 mM tBuOOH (open triangles), or 0.2 mM tBuOOH (filled inverted triangles) for the indicated times. Each data point represents the average of three technical triplicates for quantitative PCR from one biological replicate of treated cells. The symbol for the untreated cultures (time 0) represents the overlap of all three symbols used. *B*, transcript abundance of genes encoding enzymes of the L-galactose pathway quantified by RNA-Seq in *C. reinhardtii* cells grown in the presence of 1 mM H_2O_2 for 30 min (open circles) or 60 min (filled circles). Fold-changes were calculated relative to the transcript abundances in untreated cells for both quantitative PCR and RNA-Seq experiments.

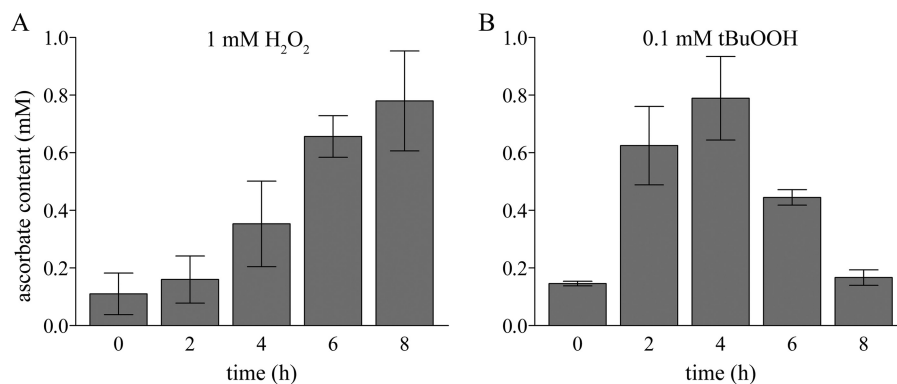


FIGURE 5. Ascorbate levels are elevated in response to oxidative stress. Vitamin C concentration was measured in extracts of *C. reinhardtii* cells exposed to 1 mM H_2O_2 (*A*) or 0.1 mM tBuOOH (*B*) for 2, 4, 6, and 8 h. Error bars represent the S.D. from three biological replicates.

mM H_2O_2 or 0.1–0.2 mM tBuOOH for 30, 60, 120, or 240 min. In plants, and most likely also in *C. reinhardtii*, Photosystem I is the major site for superoxide anion production (O_2^-) (17), which is disproportionated to H_2O_2 by the action of one or several superoxide dismutases. Here we found that in *C. reinhardtii*, *MSD3* transcript levels (encoding plastid-localized MnSOD3) are highly induced in response to peroxide treatment (Fig. 6A). Treatment of *C. reinhardtii* cells with 1 mM H_2O_2 resulted in a 2–15-fold induction of this gene over the 4-h exposure period. An even higher level of up-regulation (100-fold after 60 min) was reached when *C. reinhardtii* cells were exposed to 0.1 mM tBuOOH. H_2O_2 produced by MnSOD3 is reduced to H_2O by ascorbate in a reaction catalyzed by APX1. The mRNA abundance of *C. reinhardtii* APX1 was induced 2–4-fold after exposure to 1 mM H_2O_2 , whereas 0.1 mM tBuOOH treatment resulted in a 10–15-fold induction of APX1 transcript levels (Fig. 6A). Ascorbate peroxidase oxidizes ascorbate to monodehydroascorbate, which is either reduced to ascorbate by the action of MDAR1, or spontaneously disproportionates to dehydroascorbate. MDAR1 mRNA abundance was induced in response to 1 mM H_2O_2 (5–6-fold after 120 min), whereas 0.1 mM tBuOOH treatment resulted in a more subtle 2–3-fold up-regulation of this gene. Dehydroascorbate can be reduced back to ascorbate by DHAR1. The reaction requires reduced GSH.

The resulting oxidized GSSG is converted back to GSH by glutathione reductases (GSHR1/2 in *C. reinhardtii*). *DHAR1* transcript abundance was progressively up-regulated after exposure to 1 mM H_2O_2 (from 2–3-fold after 30 min to 50-fold after 240 min). A similar trend of *DHAR1* overexpression was observed under tBuOOH treatment (Fig. 6A). The transcript levels of the key enzyme involved in glutathione synthesis, γ -glutamylcysteine synthetase (*GSH1*), and GSHR1 were induced only in response to 1 mM H_2O_2 (Fig. 6A). Interestingly, neither of those transcripts changed in abundance during the first 60 min after 0.1 or 0.2 mM tBuOOH addition and in fact they even decreased after 120 min (Fig. 6A). RNA-Seq analysis of *C. reinhardtii* cells exposed to 1 mM H_2O_2 for 30 and 60 min indicated up-regulation of all the genes encoding the enzymes of the ascorbate-glutathione cycle (Fig. 6B and supplemental Table S3). The increase in their transcript abundance was higher after 60 min and, in agreement with the real-time PCR results, *MSD3* and *DHAR1* were the most highly induced genes. We conclude, based on the transcript abundance changes observed in this study in response to peroxide stress, that the ascorbate-glutathione system plays an important role in the oxidative stress response in *C. reinhardtii*.

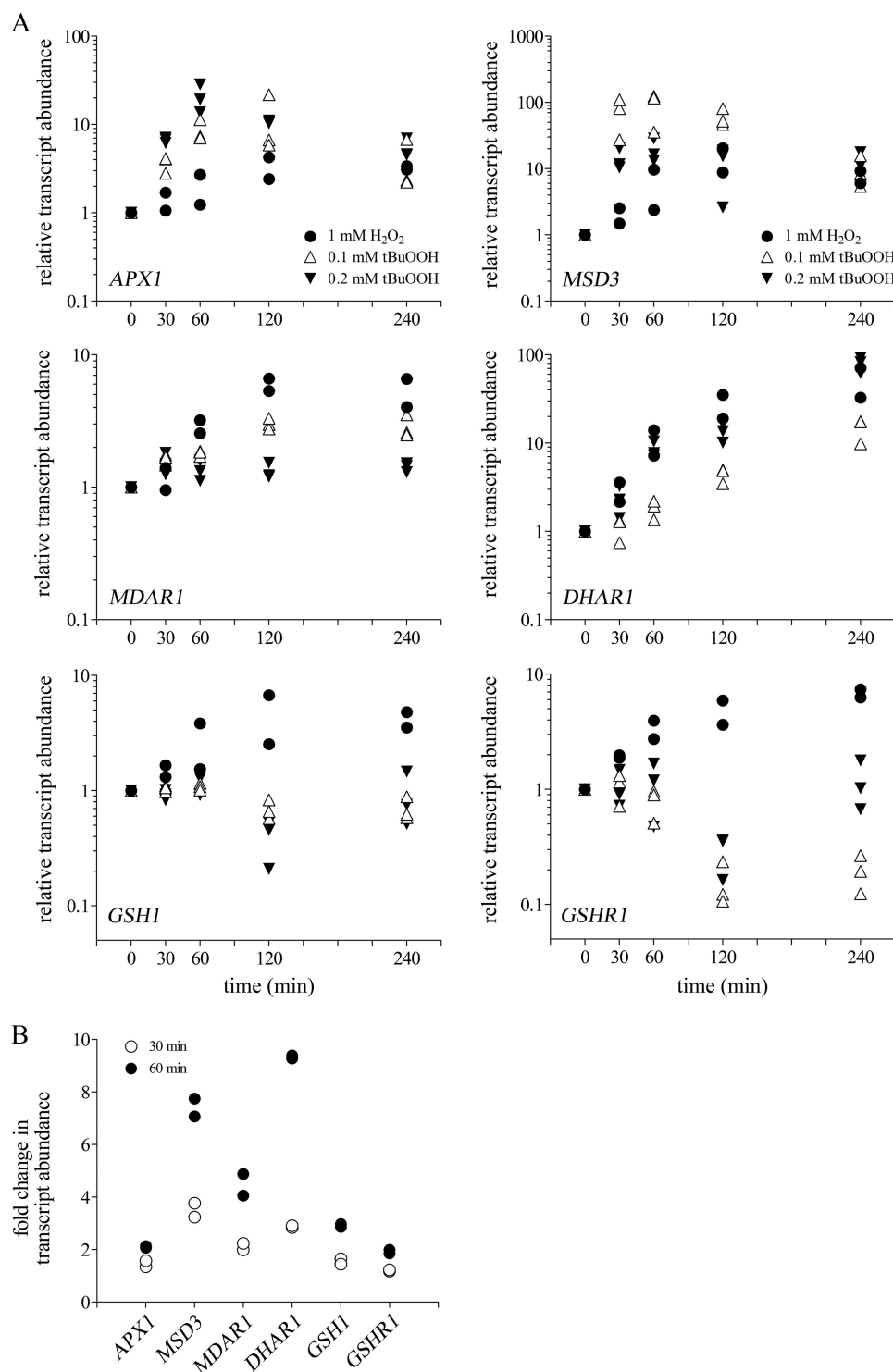


FIGURE 6. **Oxidative stress conditions result in up-regulation of GSH-ascorbate cycle enzymes.** *A*, relative transcript levels of genes coding for ascorbate-glutathione cycle components were quantified by real-time PCR in *C. reinhardtii* cells grown in the presence of 1 mM H₂O₂ (filled circles), 0.1 mM tBuOOH (open triangles), or 0.2 mM tBuOOH (filled inverted triangles) for 30, 60, 120, and 240 min. Fold-changes were calculated relative to the transcripts abundance in untreated cells and data are represented in the log₁₀ scale. Relative transcript abundance was calculated as described in the legend of Fig. 4A. Each data point represents the average of three technical triplicates from one biological replicate. *B*, RNA-Seq was also used to measure transcript levels of genes encoding for enzymes of the ascorbate-glutathione system in *C. reinhardtii* cells exposed to 1 mM H₂O₂ for 30 and 60 min.

DISCUSSION

Higher plants synthesize L-ascorbic acid using primarily the Smirnoff-Wheeler pathway (4, 9), in which VTC2 catalyzes a rate-limiting step by converting GDP-L-galactose to L-galactose-1-P (5, 8). Here we provide evidence that *C. reinhardtii* and

other green algal genomes encode functional plant VTC2 homologs. Our sequence analyses identified orthologs of all the Smirnoff-Wheeler pathway enzymes in *C. reinhardtii*. Moreover, with the exception of GDP-D-mannose pyrophosphorylase (VTC1), which appears to be missing in Prasinophyceae

Ascorbate Biosynthesis and Regulation in *Chlamydomonas*

like *Micromonas* spp. or *Ostreococcus* spp., all other enzymes of the L-galactose pathway are conserved in divergent green algae. The absence of VTC1 in Prasinophyceae might be compensated by the operation, in those species, of VTC2 cycles such as those proposed by Laing *et al.* (6) or Wolucka and Van Montagu (47), where L-galactose-1-P would be formed by a GDP-L-galactose transferase activity of VTC2 (using D-Man-1-P or D-Glc-1-P as guanylyl acceptors instead of P_i) and GDP-D-mannose formation would be ensured by a hypothetical 2'-epimerase from GDP-D-glucose (8).

HIT proteins are members of a superfamily of nucleotide hydrolases and transferases, which, based on sequence, substrate specificity, structure, evolution and mechanism, are classified into the Hint, Fhit, Aprataxin, scavenger decapping protein, and GalT branches (16). The first four branches, characterized by a HXHXH motif, contain nucleotide hydrolases, whereas GalT branch members, generally possessing a HXHXQ motif, are nucleotide phosphorylases or transferases. The best-characterized member of the GalT branch is galactose-1-phosphate uridylyltransferase, which represents the second enzyme in the Leloir pathway of galactose utilization. The HIT motif in *A. thaliana* and other plant VTC2 proteins (HXHXQ) and the enzymatic properties of *A. thaliana* VTC2, which is a GDP-L-Gal/GDP-D-Glc phosphorylase, would place this protein in the GalT branch of the HIT superfamily. Interestingly, *C. reinhardtii* VTC2 possesses the HXHXH motif found in members of the hydrolase branches of the HIT superfamily (16). Animal homologs of plant VTC2 also have the HXHXH motif and have been shown to act as specific GDP-D-glucose phosphorylases needed for quality control of the nucleoside diphosphate sugar pool (48). This work provides an additional example to suggest that the HXHXH *versus* HXHXQ motifs do not always predict the biochemical reaction catalyzed by the corresponding HIT enzyme (48–50). In this study we indeed showed that the recombinant *C. reinhardtii* VTC2 enzyme has a GDP-L-Gal/GDP-D-Glc phosphorylase activity as do the land plant homologs. The algal enzyme can use both GDP-L-Gal and GDP-D-Glc as substrates and requires inorganic phosphate as acceptor. The recombinant purified enzyme displayed an about 10-fold higher catalytic efficiency with both nucleotide sugar substrates relative to *A. thaliana* VTC2. The latter was previously found to exhibit some transferase activity (31), and we also detected a minor GDP-L-galactose transferase activity with D-Glc-1-P as a guanylyl acceptor for recombinant *C. reinhardtii* VTC2. This transferase activity was at least 100-fold lower than its phosphorylase activity (data not shown).

L-Ascorbic acid is a major antioxidant in plants and animals (46). In plants, cellular L-ascorbic levels are increased in response to environmental stresses such as high light (1, 51), high temperature (52), and exposure to UV radiation (53, 54) or ozone (55, 56). L-Ascorbic acid plays an important role in photosynthesis where it acts by scavenging superoxide and H₂O₂, participates in regeneration of α -tocopherol radicals produced by α -tocopherol during reduction of lipid peroxyl radicals, and functions as cofactor for violaxanthin de-epoxidase (1) and prolyl hydroxylases (2, 3).

Here we provide evidence suggesting a role of L-ascorbic acid in protecting *C. reinhardtii* cells against oxidative stress. Reactive oxygen species-inducing chemicals like H₂O₂ and tBuOOH resulted in increased VTC2 mRNA levels, which are 10–15 times more abundant after exposure to tBuOOH compared with H₂O₂ treatment. This might be explained by the fact that tBuOOH persists for a longer time than does H₂O₂ in liquid cultures. In addition, H₂O₂ can produce highly reactive hydroxyl radicals, whereas tBuOOH can decompose to other alkoxy and peroxy radicals. Prooxidant effects of H₂O₂ treatment resulted in persistent elevated levels of total ascorbate, whereas, after an initial increase, the total ascorbate levels dropped back to wild-type levels after exposure to tBuOOH for 8 h. This is not surprising because exposure of astrocytes, hepatocytes, or Hep2G cells to tBuOOH had previously been shown to lead to decreased levels of intracellular L-ascorbic acid and GSH (44, 45, 57). An *A. thaliana* line (*ppr40-1*) that has impaired electron flow at complex III showed decreased levels of total ascorbate and enhanced activity of GLDH and ascorbate-glutathione cycle enzymes (58). Similarly, inhibition of mitochondrial respiratory electron transport at the levels of complex I, complex II, or complex IV resulted in a 50% decrease in total ascorbate levels in *A. thaliana* (59). It is well known that plant mitochondria are the place where the last step of vitamin C biosynthesis occurs in plants. GLDH is an inner membrane mitochondrial flavin enzyme that uses oxidized cytochrome *c* as an electron acceptor (60) and recently has been shown to be required for accumulation of complex I in *A. thaliana* (61). On the other hand, tBuOOH has been shown to inhibit mitochondrial respiratory chain enzymes in rat hepatocytes (62). Therefore the higher VTC2 transcript levels and depletion of intracellular ascorbate content in *C. reinhardtii* exposed for longer times to tBuOOH might at least in part be a result of oxidatively damaged mitochondria and impaired respiratory electron transport.

Our RNA-Seq analysis of H₂O₂ stressed *C. reinhardtii* cells indicates a significant increase in mRNA levels only for VTC2 and only a small increase (1.5–2-fold) for the other components of the L-galactose pathway. A similar pattern of expression for all genes encoding L-galactose pathway enzymes has been observed in *A. thaliana* exposed to high light (30). Our results suggest that VTC2 might be the regulatory point controlling L-ascorbate biosynthesis in *C. reinhardtii*. Supporting evidence for this also comes from studies in *A. thaliana* where it has been demonstrated that supplementation with L-ascorbate decreases VTC2 mRNA abundance, possibly indicating a feedback inhibition at the transcriptional level (30). Moreover, the increased L-ascorbate content after exposure to high-light resulted in higher GDP-L-galactose phosphorylase activity (30).

The ascorbate-glutathione cycle is the major H₂O₂ scavenging system in photosynthetic organisms (2, 17, 46) (Fig. 7). In *C. reinhardtii* the superoxide anion (O₂⁻) formed at the site of Photosystem I is converted to H₂O₂ by superoxide dismutases MnSOD3 and FeSOD. The H₂O₂ is reduced to water by ascorbate in a reaction catalyzed by APX1 (63). Oxidation of ascorbate produces monodehydroascorbate,

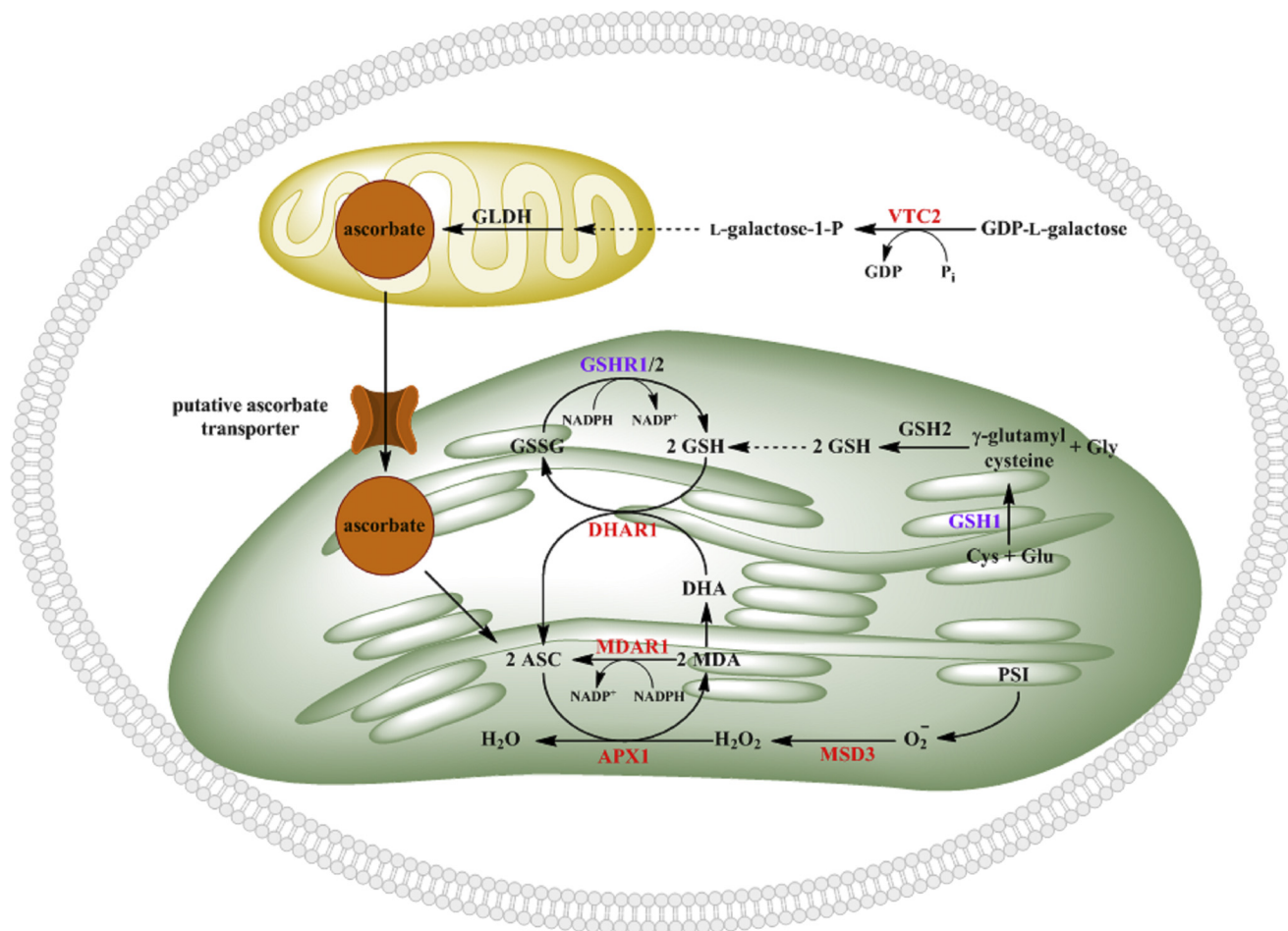


FIGURE 7. Putative regulatory sites for ascorbate biosynthesis and ascorbate recycling in *C. reinhardtii*. Enzymes depicted in red indicate the proteins whose mRNA levels are increased in response to oxidative stress (1 mM H₂O₂ and 0.1 mM tBuOOH) and those in magenta that show changes in mRNA levels only in response to H₂O₂ treatment. APX1 (ascorbate peroxidase), MSD3 (Mn superoxide dismutase), MDAR1 (monodehydroascorbate reductase), DHAR1 (dehydroascorbate reductase), GSH1 (γ -glutamylcysteine synthetase), GSH2 (glutathione synthetase), GSHR1/2 (glutathione reductase), GLDH (L-galactono-1,4-lactone dehydrogenase), VTC2 (GDP-L-galactose phosphorylase), ASC (ascorbate), MDA (monodehydroascorbate), and DHA (dehydroascorbate) are indicated.

which either can be reduced to ascorbate by MDAR1 or can spontaneously disproportionate to dehydroascorbate. DHAR1 uses GSH to regenerate ascorbate from dehydroascorbate and GSHR1/2 regenerates GSH from GSSG. It has been demonstrated that overexpression of *A. thaliana* or tomato (*Lycopersicon esculentum* Mill) monodehydroascorbate reductase (64, 65) results in increased ascorbate levels. Similarly, overexpression of dehydroascorbate reductase had the same effect in enhancing the plant vitamin C content, conferring increased tolerance to oxidative stress (66, 67). In this study, oxidatively stressed *C. reinhardtii* cells showed enhanced mRNA abundance for all transcripts encoding the ascorbate-glutathione components. An interesting observation was that exposure of *C. reinhardtii* cells to tBuOOH did not induce glutathione synthesis (*GSH1*) or GSSG reduction (*GSHR1/2*), suggesting that under these conditions, another (glutathione-independent) mechanism is required for dehydroascorbate reduction. A similar mechanism has been observed to be functional in rat liver where a selenoenzyme thioredoxin reductase reduces dehydroascorbate to ascorbate (68). *C. reinhardtii*, unlike land plants, has

selenoenzymes, including a thioredoxin reductase prototype (69, 70).

Acknowledgments—We thank Prof. Shinichi Kitamura (Osaka Prefecture University) for kindly providing GDP-L-galactose and Annie Shin for help with the expression and purification of recombinant VTC2.

REFERENCES

- Smirnoff, N. (2000) Ascorbate biosynthesis and function in photoprotection. *Philos. Trans. R. Soc. Lond. B Biol. Sci.* **355**, 1455–1464
- Gill, S. S., and Tuteja, N. (2010) Reactive oxygen species and antioxidant machinery in abiotic stress tolerance in crop plants. *Plant Physiol. Biochem.* **48**, 909–930
- Smirnoff, N., and Wheeler, G. L. (2000) Ascorbic acid in plants. Biosynthesis and function. *Crit. Rev. Biochem. Mol. Biol.* **35**, 291–314
- Wheeler, G. L., Jones, M. A., and Smirnoff, N. (1998) The biosynthetic pathway of vitamin C in higher plants. *Nature* **393**, 365–369
- Linster, C. L., Gomez, T. A., Christensen, K. C., Adler, L. N., Young, B. D., Brenner, C., and Clarke, S. G. (2007) *Arabidopsis* VTC2 encodes a GDP-L-galactose phosphorylase, the last unknown enzyme in the Smirnoff-Wheeler pathway to ascorbic acid in plants. *J. Biol. Chem.* **282**, 18879–18885

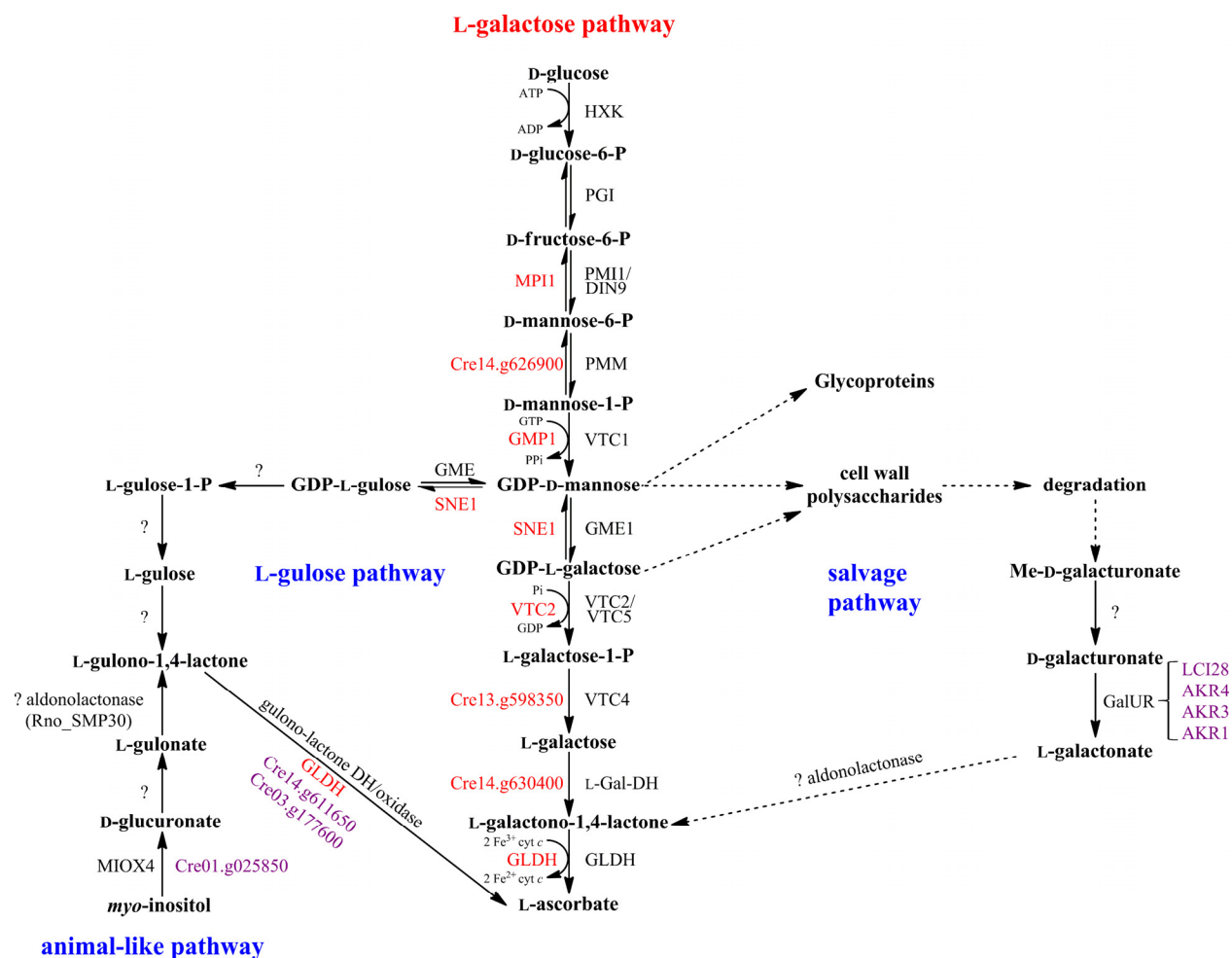
6. Laing, W. A., Wright, M. A., Cooney, J., and Bulley, S. M. (2007) The missing step of the L-galactose pathway of ascorbate biosynthesis in plants, an L-galactose guanyltransferase, increases leaf ascorbate content. *Proc. Natl. Acad. Sci. U.S.A.* **104**, 9534–9539
7. Hancock, R. D., and Viola, R. (2005) Biosynthesis and catabolism in L-ascorbic acid in plants. *Crit. Rev. Plant Sci.* **24**, 167–188
8. Linster, C. L., and Clarke, S. G. (2008) L-Ascorbate biosynthesis in higher plants. The role of VTC2. *Trends Plant Sci.* **13**, 567–573
9. Smirnoff, N., Conklin, P. L., and Loewus, F. A. (2001) Biosynthesis of ascorbic acid in plants. A renaissance. *Annu. Rev. Plant Physiol. Plant Mol. Biol.* **52**, 437–467
10. Di Matteo, A., Hancock, R. D., Ross, H. A., Frusciante, L., and Viola, R. (2003) Characterization of *Chlorella pyrenoidosa* L-ascorbic acid accumulating mutants. Identification of an enhanced biosynthetic enzyme activity and cloning of the putative gene from *Arabidopsis thaliana*. *Comp. Biochem. Physiol. A* **134**, S155
11. Renstrom, B., Grün, M., and Loewus, F. (1982) Biosynthesis of L-ascorbic acid in *Chlorella pyrenoidosa*. *Plant Cell Lett.* **28**, 299–305
12. Running, J. A., Burlingame, R. P., and Berry, A. (2003) The pathway of L-ascorbic acid biosynthesis in the colourless microalga *Prototheca moriformis*. *J. Exp. Bot.* **54**, 1841–1849
13. Helsper, J. P., Kagan, L., Hilby, C. L., Maynard, T. M., and Loewus, F. A. (1982) L-Ascorbic acid biosynthesis in *Ochromonas danica*. *Plant Physiol.* **69**, 465–468
14. Shigeoka, S., Nakano, Y., and Kitaoka, S. (1979) The biosynthetic pathway of L-ascorbic acid in *Euglena gracilis* Z. *J. Nutr. Sci. Vitaminol.* **25**, 299–307
15. Grün, M., and Loewus, F. A. (1984) L-Ascorbic acid biosynthesis in the euryhaline diatom *Cyclotella cryptica*. *Planta* **160**, 6–11
16. Brenner, C. (2007) in *Encyclopedia of Life Sciences*, pp. 1–6, John Wiley & Sons, Ltd., Chichester, UK
17. Asada, K. (1999) The water-water cycle in chloroplasts. Scavenging of active oxygens and dissipation of excess photons. *Annu. Rev. Plant Physiol. Plant Mol. Biol.* **50**, 601–639
18. Watanabe, K., Suzuki, K., and Kitamura, S. (2006) Characterization of a GDP-D-mannose 3',5'-epimerase from rice. *Phytochemistry* **67**, 338–346
19. Harris, E. H. (2009) *The Chlamydomonas Sourcebook, A Comprehensive Guide to Biology and Laboratory Use*, 2nd Ed., Academic Press, San Diego
20. Fox, J. D., and Waugh, D. S. (2003) Maltose-binding protein as a solubility enhancer. *Methods Mol. Biol.* **205**, 99–117
21. Quinn, J. M., and Merchant, S. (1998) Copper-responsive gene expression during adaptation to copper deficiency. *Methods Enzymol.* **297**, 263–279
22. Allen, M. D., del Campo, J. A., Kropat, J., and Merchant, S. S. (2007) FEA1, FEA2, and FRE1, encoding two homologous secreted proteins and a candidate ferrireductase, are expressed coordinately with FOX1 and FTR1 in iron-deficient *Chlamydomonas reinhardtii*. *Eukaryot. Cell* **6**, 1841–1852
23. Schloss, J. A. (1990) A *Chlamydomonas* gene encodes a G protein β subunit-like polypeptide. *Mol. Gen. Genet.* **221**, 443–452
24. Craigie, R. A., and Cavalier-Smith, T. (1982) Cell volume and the control of the *Chlamydomonas* cell cycle. *J. Cell Sci.* **54**, 173–191
25. Langmead, B., Trapnell, C., Pop, M., and Salzberg, S. L. (2009) Ultrafast and memory-efficient alignment of short DNA sequences to the human genome. *Genome Biol.* **10**, R25
26. Mortazavi, A., Williams, B. A., McCue, K., Schaeffer, L., and Wold, B. (2008) Mapping and quantifying mammalian transcriptomes by RNA-Seq. *Nat. Methods* **5**, 621–628
27. Castruita, M., Casero, D., Karpowicz, S. J., Kropat, J., Vieler, A., Hsieh, S. I., Yan, W., Cokus, S., Loo, J. A., Benning, C., Pellegrini, M., and Merchant, S. S. (2011) Systems biology approach in *Chlamydomonas* reveals connections between copper nutrition and multiple metabolic steps. *Plant Cell* **23**, 1273–1292
28. Whelan, S., and Goldman, N. (2001) A general empirical model of protein evolution derived from multiple protein families using a maximum-likelihood approach. *Mol. Biol. Evol.* **18**, 691–699
29. Tamura, K., Peterson, D., Peterson, N., Stecher, G., Nei, M., and Kumar, S. (2011) MEGA5. Molecular evolutionary genetics analysis using maximum likelihood, evolutionary distance, and maximum parsimony methods. *Mol. Biol. Evol.* **28**, 2731–2739
30. Dowdle, J., Ishikawa, T., Gatzek, S., Rolinski, S., and Smirnoff, N. (2007) Two genes in *Arabidopsis thaliana* encoding GDP-L-galactose phosphorylase are required for ascorbate biosynthesis and seedling viability. *Plant J.* **52**, 673–689
31. Linster, C. L., Adler, L. N., Webb, K., Christensen, K. C., Brenner, C., and Clarke, S. G. (2008) A second GDP-L-galactose phosphorylase in *Arabidopsis en route* to vitamin C. Covalent intermediate and substrate requirements for the conserved reaction. *J. Biol. Chem.* **283**, 18483–18492
32. Ishikawa, T., and Shigeoka, S. (2008) Recent advances in ascorbate biosynthesis and the physiological significance of ascorbate peroxidase in photosynthesizing organisms. *Biosci. Biotechnol. Biochem.* **72**, 1143–1154
33. Wolucka, B. A., and Van Montagu, M. (2003) GDP-mannose 3',5'-epimerase forms GDP-L-gulose, a putative intermediate for the *de novo* biosynthesis of vitamin C in plants. *J. Biol. Chem.* **278**, 47483–47490
34. Radzio, J. A., Lorence, A., Chevone, B. I., and Nessler, C. L. (2003) L-Gulonono-1,4-lactone oxidase expression rescues vitamin C-deficient *Arabidopsis* (*vtc*) mutants. *Plant Mol. Biol.* **53**, 837–844
35. Linster, C. L., and Van Schaftingen, E. (2007) Vitamin C. Biosynthesis, recycling, and degradation in mammals. *FEBS J.* **274**, 1–22
36. Kondo, Y., Inai, Y., Sato, Y., Handa, S., Kubo, S., Shimokado, K., Goto, S., Nishikimi, M., Maruyama, N., and Ishigami, A. (2006) Senescence marker protein 30 functions as gluconolactonase in L-ascorbic acid biosynthesis, and its knockout mice are prone to scurvy. *Proc. Natl. Acad. Sci. U.S.A.* **103**, 5723–5728
37. Agius, F., González-Lamothe, R., Caballero, J. L., Muñoz-Blanco, J., Bottella, M. A., and Valpuesta, V. (2003) Engineering increased vitamin C levels in plants by overexpression of a D-galacturonic acid reductase. *Nat. Biotechnol.* **21**, 177–181
38. Ishikawa, T., Nishikawa, H., Gao, Y., Sawa, Y., Shibata, H., Yabuta, Y., Maruta, T., and Shigeoka, S. (2008) The pathway via D-galacturonate/L-galactonate is significant for ascorbate biosynthesis in *Euglena gracilis*. Identification and functional characterization of aldonolactonase. *J. Biol. Chem.* **283**, 31133–31141
39. Müller-Moulé, P. (2008) An expression analysis of the ascorbate biosynthesis enzyme VTC2. *Plant Mol. Biol.* **68**, 31–41
40. Allen, M. D., Kropat, J., Tottey, S., Del Campo, J. A., and Merchant, S. S. (2007) Manganese deficiency in *Chlamydomonas* results in loss of photosystem II and MnSOD function, sensitivity to peroxides, and secondary phosphorus and iron deficiency. *Plant Physiol.* **143**, 263–277
41. Fischer, B. B., Eggen, R. I., and Niyogi, K. K. (2010) Characterization of single oxygen-accumulating mutants isolated in a screen for altered oxidative stress response in *Chlamydomonas reinhardtii*. *BMC Plant Biol.* **10**, 279
42. Ledford, H. K., Chin, B. L., and Niyogi, K. K. (2007) Acclimation to singlet oxygen stress in *Chlamydomonas reinhardtii*. *Eukaryot. Cell* **6**, 919–930
43. Long, J. C., and Merchant, S. S. (2008) Photooxidative stress impacts the expression of genes encoding iron metabolism components in *Chlamydomonas*. *Photochem. Photobiol.* **84**, 1395–1403
44. Glascock, P. A., Jr., Gilfor, E., and Farber, J. L. (1995) Relationship of the metabolism of vitamins C and E in cultured hepatocytes treated with *tert*-butyl hydroperoxide. *Mol. Pharmacol.* **48**, 80–88
45. Daskalopoulos, R., Korcok, J., Tao, L., and Wilson, J. X. (2002) Accumulation of intracellular ascorbate from dehydroascorbic acid by astrocytes is decreased after oxidative stress and restored by propofol. *Glia* **39**, 124–132
46. Foyer, C. H., and Noctor, G. (2011) Ascorbate and glutathione. The heart of the redox hub. *Plant Physiol.* **155**, 2–18
47. Wolucka, B. A., and Van Montagu, M. (2007) The VTC2 cycle and the *de novo* biosynthesis pathways for vitamin C in plants. An opinion. *Phytochemistry* **68**, 2602–2613
48. Adler, L. N., Gomez, T. A., Clarke, S. G., and Linster, C. L. (2011) A novel GDP-D-glucose phosphorylase involved in quality control of the nucleoside diphosphate sugar pool in *Caenorhabditis elegans* and mammals. *J. Biol. Chem.* **286**, 21511–21523
49. Guranowski, A., Wojdyła, A. M., Zimny, J., Wypijewska, A., Kowalska, J., Jemielity, J., Davis, R. E., and Bieganski, P. (2010) Dual activity of certain HIT-proteins. *A. thaliana* Hint4 and *C. elegans* DcpS act on adenosine 5'-phosphosulfate as hydrolases (forming AMP) and as phosphorylases

- (forming ADP). *FEBS Lett.* **584**, 93–98
50. Mori, S., Shibayama, K., Wachino, J., and Arakawa, Y. (2010) Purification and molecular characterization of a novel diadenosine 5',5'''-P(1),P(4)-tetrakisphosphate phosphorylase from *Mycobacterium tuberculosis* H37Rv. *Protein Expr. Purif.* **69**, 99–105
 51. Müller-Moulé, P., Golan, T., and Niyogi, K. K. (2004) Ascorbate-deficient mutants of *Arabidopsis* grow in high light despite chronic photooxidative stress. *Plant Physiol.* **134**, 1163–1172
 52. Larkindale, J., Hall, J. D., Knight, M. R., and Vierling, E. (2005) Heat stress phenotypes of *Arabidopsis* mutants implicate multiple signaling pathways in the acquisition of thermotolerance. *Plant Physiol.* **138**, 882–897
 53. Conklin, P. L., Williams, E. H., and Last, R. L. (1996) Environmental stress sensitivity of an ascorbic acid-deficient *Arabidopsis* mutant. *Proc. Natl. Acad. Sci. U.S.A.* **93**, 9970–9974
 54. Filkowski, J., Kovalchuk, O., and Kovalchuk, I. (2004) Genome stability of *vtc1*, *tt4*, and *tt5* *Arabidopsis thaliana* mutants impaired in protection against oxidative stress. *Plant J.* **38**, 60–69
 55. Chen, Z., and Gallie, D. R. (2005) Increasing tolerance to ozone by elevating foliar ascorbic acid confers greater protection against ozone than increasing avoidance. *Plant Physiol.* **138**, 1673–1689
 56. Sanmartin, M., Drogoudi, P. A., Lyons, T., Pateraki, I., Barnes, J., and Kanellis, A. K. (2003) Overexpression of ascorbate oxidase in the apoplast of transgenic tobacco results in altered ascorbate and glutathione redox states and increased sensitivity to ozone. *Planta* **216**, 918–928
 57. Alía, M., Ramos, S., Mateos, R., Bravo, L., and Goya, L. (2005) Response of the antioxidant defense system to *tert*-butyl hydroperoxide and hydrogen peroxide in a human hepatoma cell line (HepG2). *J. Biochem. Mol. Toxicol.* **19**, 119–128
 58. Zsigmond, L., Tomasskovic, B., Deák, V., Rigó, G., Szabados, L., Bánhegyi, G., and Szarka, A. (2011) Enhanced activity of galactono-1,4-lactone dehydrogenase and ascorbate-glutathione cycle in mitochondria from complex III-deficient *Arabidopsis*. *Plant Physiol. Biochem.* **49**, 809–815
 59. Yabuta, Y., Maruta, T., Nakamura, A., Mieda, T., Yoshimura, K., Ishikawa, T., and Shigeoka, S. (2008) Conversion of L-galactono-1,4-lactone to L-ascorbate is regulated by the photosynthetic electron transport chain in *Arabidopsis*. *Biosci. Biotechnol. Biochem.* **72**, 2598–2607
 60. Leferink, N. G., van den Berg, W. A., and van Berkel, W. J. (2008) L-Galactono- γ -lactone dehydrogenase from *Arabidopsis thaliana*, a flavoprotein involved in vitamin C biosynthesis. *FEBS J.* **275**, 713–726
 61. Pineau, B., Layoune, O., Danon, A., and De Paepe, R. (2008) L-Galactono-1,4-lactone dehydrogenase is required for the accumulation of plant respiratory complex I. *J. Biol. Chem.* **283**, 32500–32505
 62. Drahota, Z., Kriváková, P., Cervinková, Z., Kmoníková, E., Lotková, H., Kucera, O., and Houstek, J. (2005) *tert*-Butyl hydroperoxide selectively inhibits mitochondrial respiratory chain enzymes in isolated rat hepatocytes. *Physiol. Res.* **54**, 67–72
 63. Takeda, T., Ishikawa, T., and Shigeoka, S. (1997) Metabolism of hydrogen peroxide by the scavenging system in *Chlamydomonas reinhardtii*. *Physiol. Plant* **99**, 49–55
 64. Eltayeb, A. E., Kawano, N., Badawi, G. H., Kaminaka, H., Sanekata, T., Shibahara, T., Inanaga, S., and Tanaka, K. (2007) Overexpression of monodehydroascorbate reductase in transgenic tobacco confers enhanced tolerance to ozone, salt and polyethylene glycol stresses. *Planta* **225**, 1255–1264
 65. Li, F., Wu, Q. Y., Sun, Y. L., Wang, L. Y., Yang, X. H., and Meng, Q. W. (2010) Overexpression of chloroplastic monodehydroascorbate reductase enhanced tolerance to temperature and methyl viologen-mediated oxidative stresses. *Physiol. Plant* **139**, 421–434
 66. Chen, Z., Young, T. E., Ling, J., Chang, S. C., and Gallie, D. R. (2003) Increasing vitamin C content of plants through enhanced ascorbate recycling. *Proc. Natl. Acad. Sci. U.S.A.* **100**, 3525–3530
 67. Wang, Z., Xiao, Y., Chen, W., Tang, K., and Zhang, L. (2010) Increased vitamin C content accompanied by an enhanced recycling pathway confers oxidative stress tolerance in *Arabidopsis*. *J. Integr. Plant Biol.* **52**, 400–409
 68. May, J. M., Mendiratta, S., Hill, K. E., and Burk, R. F. (1997) Reduction of dehydroascorbate to ascorbate by the selenoenzyme thioredoxin reductase. *J. Biol. Chem.* **272**, 22607–22610
 69. Novoselov, S. V., and Gladyshev, V. N. (2003) Non-animal origin of animal thioredoxin reductases. Implications for selenocysteine evolution and evolution of protein function through carboxyl-terminal extensions. *Protein Sci.* **12**, 372–378
 70. Novoselov, S. V., Rao, M., Onoshko, N. V., Zhi, H., Kryukov, G. V., Xiang, Y., Weeks, D. P., Hatfield, D. L., and Gladyshev, V. N. (2002) Selenoproteins and selenocysteine insertion system in the model plant cell system, *Chlamydomonas reinhardtii*. *EMBO J.* **21**, 3681–3693

SUPPLEMENTAL MATERIALS FOR:

Impact of oxidative stress on ascorbate biosynthesis in *Chlamydomonas* via regulation of the *VTC2* gene encoding a GDP-L-galactose phosphorylase

Eugen I. Urzica, Lital N. Adler, M. Dudley Page, Carole L. Linster, Mark A. Arbing, David Casero, Matteo Pellegrini, Sabeeha S. Merchant and Steven G. Clarke



SUPPLEMENTAL FIGURE S1. Proposed biosynthetic pathways for ascorbate biosynthesis in higher plants and algae. *C. reinhardtii* orthologs of the major ascorbate biosynthetic route enzymes (L-galactose pathway) are depicted in red. MPI1 (mannose-6-phosphate isomerase), Cre14.g626900 (phosphomannomutase), GMP1 (GDP-L-mannose pyrophosphorylase), SNE1 (sugar nucleotide epimerase), VTC2 (GDP-L-galactose phosphorylase), Cre13.g598350 (L-galactose-1-P phosphatase), Cre14.g630400 (L-galactose dehydrogenase) and GLDH (L-galactono-1,4-lactone dehydrogenase). Alternative ascorbate biosynthetic pathways have been proposed (in blue), but many reaction steps have either not been identified (question marks) or the *C. reinhardtii* genome does not possess orthologs of previously characterized genes (homologs are depicted in magenta).

Ascorbate biosynthesis and regulation in *Chlamydomonas*

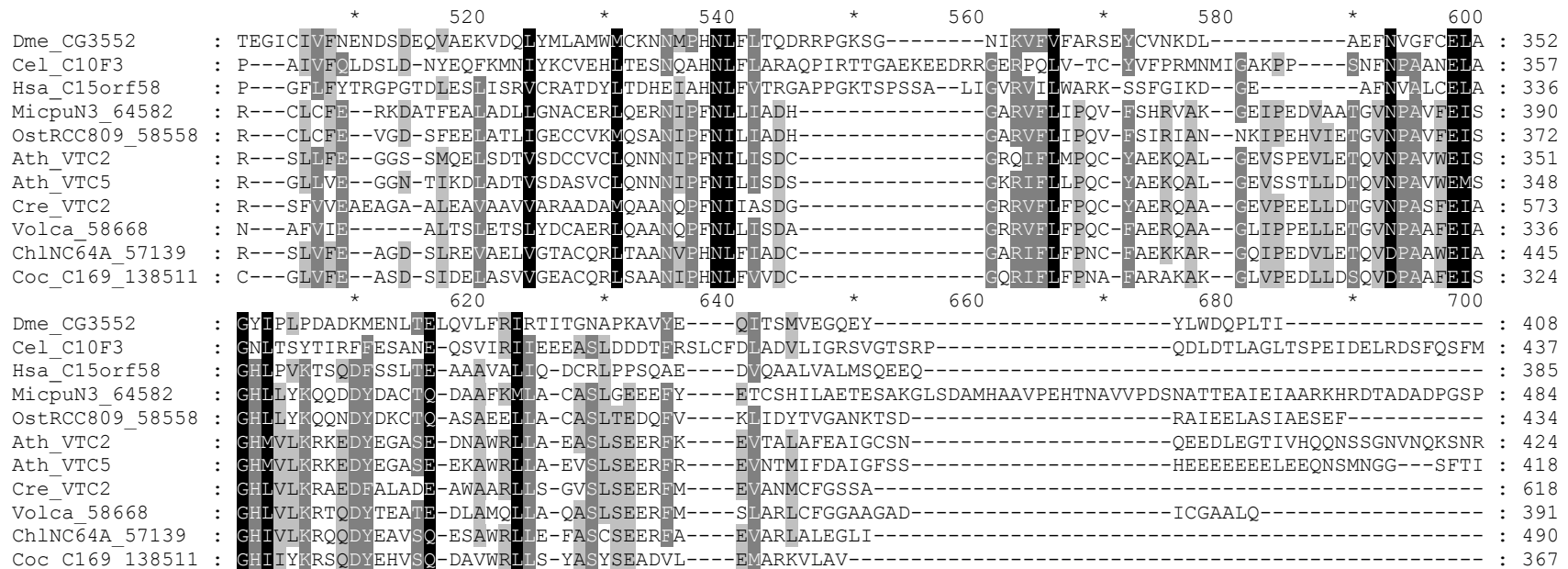
```

                *           220           *           240           *           260           *           280           *           300
Dme	CG3552	: -----MSKVKYETSLEGRAQLYLNAMKVRWDQLHKVPGLFPSYQLEKSPQSRKIFGYWGFVAELNSDRNRKRRRQ--TIESL	: 141
Cel_C10F3	: -----IYENGNSNHEKDEKALKELHERWENAKQY-NAFNYP LN-CM-YRCLDCKYDLSMOLNIERGE LRRKPMHFK--NI	: 128
Hsa_C15orf58	: -----WPRNAPGIPDALPQSPFDAALCSAWKQRVEL-GLFRYRLRELQ-TQILPGAVGFVAQLNVERG-VQRRPFC-TIKSV	: 115
MicpuN3_64582	: -----DSDSFSGGGYVDVSPFDRIILAAWEDRFAA-GLFRYDVTACK-TKVVPGGYGFVAQFNEGRA-TKKRPTEFAVDEV	: 159
OstRCC809_58558	: -----DLDSWGITGYVTDASEFDRIILISAWEDRFAG-GLFRYDVTTVS-TKVIIECTKKYVAQFNIGRA-TNKRPTFRVQDV	: 143
Ath_VTC2	: -----SHEAIEPPVAFLESLVVLGEWEDRFQR-GLFRYDVTACE-TKVIIPGKYGFVAQLNEGRH-LKKRPTEFRVDRV	: 127
Ath_VTC5	: -----NLDKSVGENTESPVTFLLESLVIGEWEDRFQR-GLFRYDVTACE-TKVIIPGKYGFIAQLNEGRH-LKKRPTEFRVDRV	: 121
Cre_VTC2	: EFVRRMARRGGAGAAAAATAVSAKAAADIGGAEVPGRSLLLEGVVMALWEDRADR-GMFRYDVSQCE-TRVLPGPAGFVAQLNEGRA-TKKRPTEFSADRV	: 296
Volca_58668	: -----GKVLVPSRSLLESALMTLWEDRADR-GLFRYDVTLC-TRVLPGSRGFIAQLNEGRA-TKKRPTEVTLDLV	: 95
ChlNC64A_57139	: DDEAVSLDG-----SSDSGASQVVPQRSVLDALLGEWEDRAEA-GLFRYDVTACP-TKLVPGSYGFIAQCNEGR L-SKKRPTEFRVDLV	: 196
Coc_C169_138511	: -----APSSDSGATSLLDTVLLAEWEDRAEQ-GLFRYDVTACP-TKVVPGAYGFVAQFNEGRG-SKKRPTEFCVDQV	: 98

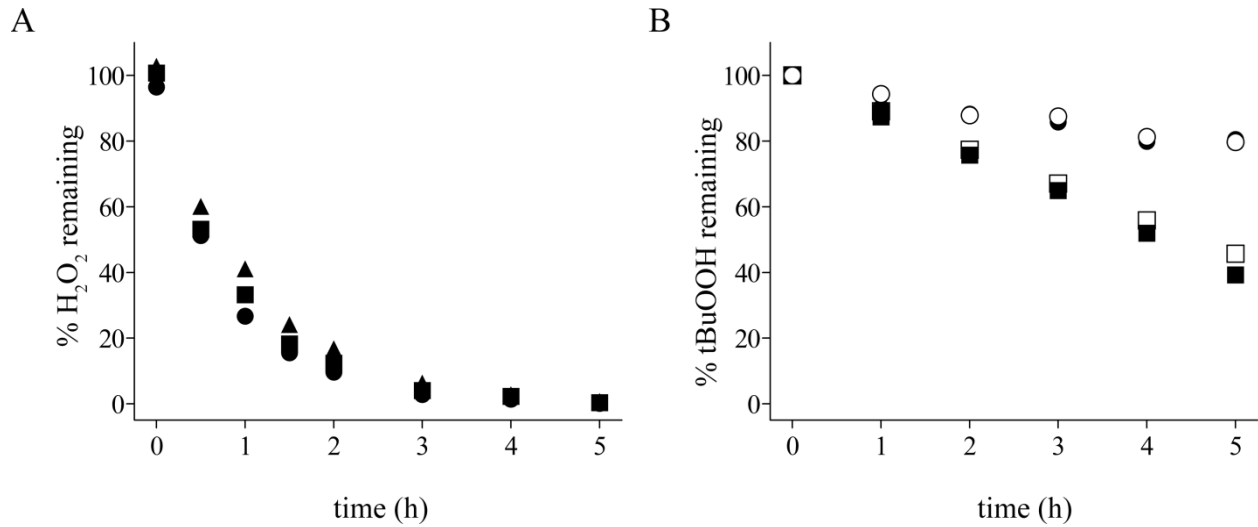
                *           320           *           340           *           360           *           380           *           400
Dme	CG3552	: NPTFKHMMFNFNKVDQAEVIMTIDDA-----HGSPVQMIINRSPITKYHTLICPEVGNKHTQRIITRDAIQ	: 207
Cel_C10F3	: KEPFNHLRFNFAKLDHDELLEYLKC-----TDFISND-----LLDRHL-VAVNASPLERDHS LIVPSV NKCSPQVLLTQAVR	: 200
Hsa_C15orf58	: ROAFDPVQFNFNKIRPGEVLERLHR-----EPDLPGLT-----LQEDIL-VVINVSPLEWGHVLLVPEPARQLPQRLLPGAR	: 187
MicpuN3_64582	: VOAFDGGKFNFTKADKAEILFAFER----GDRAMKSSA--YNSAKTI-----ESSPNV-MLINVSPIEYGHVLLCPRTDCLPQRIPEL L	: 239
OstRCC809_58558	: CQNFDPKKFNFTKADLKEVLESFTKLA-SEADKNVRSRI---FEKDAAV-----DESPTV-VLINVSPIEYGHVLLCPRTDMLPQITPGN L	: 227
Ath_VTC2	: LOSFDGSKFNFTKVGQEELLFQFEA-----GEDAQVQ---FFPCMPIDP-----ENSPSV-VAINVSPIEYGHVLLIPRVLDCLPQRI DHKSL	: 207
Ath_VTC5	: LQPF DGNKFNFTKVGQEELLFQFKAST----NDDSEIQ---FLASMP L DA-----DNSPSV-VAINVSPIEYGHVLLIPRVLDCLPQRI DHKSL	: 204
Cre_VTC2	: MOPFDPARFHNKAAMGEVLEAFQADATASATATATAAPRLLLSAPMAKSALLASNPVSGSPNL-VLINVSPIDHCHVLLVPRVLDCLPQALTPD TAL	: 395
Volca_58668	: LQPF DSAKFNFKKAAMAEALVGFPPDDAGSGGGAGGGNGGRSLLPSVAPLGA AVAA---GGSPNL-VLINVSPIDYGHVLLVPRVLDNLPQALSCGT V L	: 191
ChlNC64A_57139	: AOPYDAAKFNFTKALQQEVLEMFEPA--GGRGGRRAKPA---FRPAAPQ-----RASPNL-VYINVSPIEYGHVLLVPRALDALCOLVTPD T L	: 279
Coc_C169_138511	: VQRFNNGKFNFTKALQKEVLFQFEA-----DMSSKGS A---FLPLAPV-----SGSPNL-VFINVSPIEYGHVLLVPRALDRNLQVQPD T L K	: 178

                *           420           *           440           *           460           *           480           *           500
Dme	CG3552	: FCITFMRNIDDKD-----MRMCGYNSPGALASVNHLLHFLHLLHMPQDLYIDHVPLDEL-----AGGYVYRISRRAP	: 271
Cel_C10F3	: IAVDLMMLLVDDM-----FHILFNSILGQASVNHLLHLLHMYWYDSDLINRKCEPL-----HDVPNVYVIRPPVVIC	: 267
Hsa_C15orf58	: AGIEAVLLSLHPG-----FRVGFNSLGGLASVNHLLHLLHGYI AHRLPVEQAPSEPL-----DPGGHLLHLLQDLPA	: 252
MicpuN3_64582	: PPLYMAAESRNPY-----FRVGYNSLGAYATINHLHFCAYYIMEAFPIERAQTTRLPQRV-----YKKRHRHGVA VNVQVTGYPV	: 313
OstRCC809_58558	: PALYMAAESRNPY-----FRVGYNSLGAYATINHLHFCAYYIMEAFPIERASTAET-----FSGTHGECTVYSVNGYPV	: 296
Ath_VTC2	: LAVHMAAEANPY-----FRLGYNSLGAFATINHLHFCAYYIAMPFPLEKAPT KKI-----TTTVSGVKI SELLSYPV	: 275
Ath_VTC5	: LALQMAAEADNPY-----FRLGYNSLGAFATINHLHFCAYYIAMPFPIEKASSLKI-----TTTNGVKIKSKLLNYPV	: 272
Cre_VTC2	: LALQFAAEELGSSSSRSRSGSAFRVGYNSLGAFATINHLHFCAYYIAMPALPCE RAPTCTPLPGALARPLAASQQPRKRGAEEVAGAGSAGSVRVSRLVGY PV	: 495
Volca_58668	: LALQFAGELGN SH-----FRVGYNSLGAYATINHLHFCAYYI AKTMPCEAAATVPLPG-----VGVLGAAVRSRLVDY PV	: 263
ChlNC64A_57139	: LALQFAREADNPY-----FRLAFNSLGAYGTINHLHFCAYYI AAPYAMERAPTVPLELEGLGAGAGAGSPPPQGGK--GRRRAATGVRVDQLREY PV	: 369
Coc_C169_138511	: LALQFAHEANPY-----FRLAFNSLGAYGTVNHLLHFCAYYI AAFP AVERAPTVDL-----CCLRKYRHVRVAMLADY PV	: 248

```



SUPPLEMENTAL FIGURE S2. Sequence alignment of VTC2-like sequences. Protein sequences from *Chlamydomonas reinhardtii* (Cre), *Volvox carteri f. nagariensis* (Volca), *Micromonas* sp. RCC299 (MicpuN3), *Ostreococcus* sp. RCC809 (OstRCC809), *Chlorella* sp. NC64A (ChlNC64A), *Coccomyxa* sp. C169 (Coc_C169), *Arabidopsis thaliana* (Ath), *Drosophila melanogaster* (Dme), *Caenorhabditis elegans* (Cel) and *Homo sapiens* (Hsa) were aligned with MUSCLE at <http://www.ebi.ac.uk/Tools/msa/muscle/> and edited in GeneDoc. Back-shaded amino acids are conserved in 10 (black), 8 (dark grey), or 7 (light grey) of the aligned proteins. Histidine and glutamine residues of the HIT motif (HxHxH/Q) are highlighted in red and green, respectively. N-terminal region (200 amino acids in VTC2) with very low sequence similarities is not shown.



SUPPLEMENTAL FIGURE S3. *Tert*-butyl peroxide is more stable in *Chlamydomonas* cultures than hydrogen peroxide. A) Strain CC425 was grown in TAP to 2×10^6 cell mL⁻¹ prior to addition of H₂O₂ (1 mM). Results for three biological replicates are shown. B) Cells were grown as for (A) prior to addition of tBuOOH at concentrations of either 0.1 mM (■, □) or 0.2 mM (●, ○). Results for two biological replicates are shown.

SUPPLEMENTAL TABLE S1. Enzymes of the Smirnov-Wheeler Vitamin C biosynthesis pathway have orthologs in green algae. Protein sequences of the *A. thaliana* L-galactose pathway components, *A. thaliana* MIOX4, rat gulono-lactone oxidase and gluconolactonase (animal-like pathway), *Fragaria x ananassa* D-galacturonate reductase and *E. gracilis* aldonolactonase (salvage pathway) were used as query sequences in a BLAST search against various algal protein databases to identify homologs. ^a *Micromonas* spp. and *Ostreococcus* spp. VTC1 homologs are not mutual best hits (amino acid identity is 20-24%) (cyan) and therefore are not viewed as orthologs. Proteins marked in yellow in the salvage pathway represent mutual best hits of *Fragaria* D-galacturonate reductase. % amino acid identity is shown for *C. reinhardtii* proteins. MBH, mutual best hit.

Define	Protein ID/Name								MBH
	<i>A. thaliana</i>	<i>C. reinhardtii</i>	(% amino acid identity)	<i>Chlorella</i> sp. C64A	<i>Coccomyxa</i> sp. C169	<i>Micromonas</i> sp. RCC299	<i>O. lucimarinus</i>	<i>V. carterii</i>	
L-galactose pathway									
Phosphomannose isomerase	PMI1	Cre02.g147650/MP1	40%	139231	30417	86735	3605	65163	yes
	PMI2	Cre02.g147650/MP1	41%	139231	30417	86735	3605	65163	–
Phosphomannomutase	PMM	Cre14.g626900	72%	49345	64649	72061	39943	109528	yes
GDP-D-mannose pyrophosphorylase	VTC1	Cre16.g672800/GMP1	65%	133102	26874	59536	969	81984	yes ^a
GDP-D-mannose 3",5"-epimerase	GME1	Cre01.g019250/SNE1	74%	140350	52441	92683	18701	77112	yes
GDP-L-galactose phosphorylase	VTC2	Cre13.g588150/VTC2	46%	57139	13851	64582	3702	58668	–
	VTC5	Cre13.g588150/VTC2	47%	57139	13851	64582	3702	58668	yes
L-galactose-1-P-phosphatase	VTC4	Cre13.g598350	54%	34254	47143	79551	38679	78931	yes
L-galactose dehydrogenase	L-Gal-DH	Cre14.g630400	50%	25289	18370	59526	31498	93987	yes
L-galactono-1,4-lactone-dehydrogenase	GLDH	Cre13.g567100/GLDH	55%	28225	38144	58063	1854	88191	yes
L-gulose-pathway									
GDP-D-mannose 3",5"-epimerase	GME1	Cre01.g019250/SNE1	74%	140350	52441	92683	18701	77112	yes
Gulono-lactone oxidase (<i>Rattus norvegicus</i>)	AT3G47930	Cre13.g567100	31%				1854	88191	no
	AT2G46750	Cre03.g177600	23%	28225	38144	58063	14476	85802	
	AT2G46760	Cre14.g611650	26%						
animal-like pathway									
myo-inositol oxygenase (MIOX1)	MIOX4	Cre01.g025850	35%	–	17459	–	–	96377	no
Gulonolactonase (<i>Rattus norvegicus</i>)	–	–		136730	47480	88713	41751	–	yes
salvage pathway									
D-galacturonate reductase (<i>Fragaria x ananassa</i>)	AT1G59960	Cre02.g130950/LCI28	36%	32425	56609	86329	28670	92170	no
	AT1G59950	Cre16.g692800/AKR4	35%	138560	48592	98293	88845	108355	
	AT2G37790	Cre10.g432900/AKR3	33%	19238	14612	80447	5598	55182	
	AT2G37770	Cre19.g752450/AKR1	31%	142101	56610	84021	37521	80526	
aldonolactonase (<i>Euglena gracilis</i>)	–	–		136730	47480	88713	41751	–	yes

SUPPLEMENTAL TABLE S2. Comparison of mRNA abundances for genes encoding enzymes of the L-galactose ascorbate biosynthesis pathway in *C. reinhardtii* cells treated with 1 mM H₂O₂ for 30 and 60 minutes. ^atranscript abundance, RPKM (reads per kilobase of exon model per million mapped reads).

Protein ID Au10.2	Phytozome v7	Gene Name	Defline	RNA-Seq				
				RPKM ^a			Fold change	
				0 min	30 min	60 min	30 vs 0	60 vs 0
Cre02.g147650	19869059	<i>MPII</i>	Mannose-6-phosphate isomerase	2.7	4.6	5.6	1.7	2.1
Cre14.g626900	19860795		Phosphomannomutase	31	39	59	1.3	1.9
Cre16.g672800	19861169	<i>GMP1</i>	GDP-D-mannose pyrophosphorylase	49	66	103	1.3	2.1
Cre01.g019250	19866144	<i>SNE1</i>	sugar nucleotide epimerase	84	93	132	1.1	1.6
Cre13.g588150	19869869	<i>VTC2</i>	GDP-galactose:glucose-1-phosphate guanyltransferase	20	130	174	6.5	8.6
Cre13.g598350	19870456		Inositol-phosphate phosphatase	9.9	10	10	1.0	1.0
Cre14.g630400	19860547		Putative L-galactose dehydrogenase	11	8.9	7.8	0.83	0.72
Cre13.g567100	19870260	<i>GLDH</i>	L-galactono-1,4-lactone dehydrogenase /D-arabinono-1,4-lactone oxidase	9.8	13	16	1.3	1.6

SUPPLEMENTAL TABLE S3. Transcript abundances for genes encoding enzymes of the ascorbate-glutathione cycle after exposure to 1 mM H₂O₂ for 30 and 60 minutes. ^atranscript abundance, RPKM (reads per kilobase of exon model per million mapped reads).

Protein ID Au10.2	Phytozome v7	Gene Name	Defline	RNA-Seq				
				RPKM ^a			Fold change	
				0 min	30 min	60 min	30 vs 0	60 vs 0
Cre02.g087700	19869637	<i>APX1</i>	Ascorbate peroxidase	91	134	192	1.5	2.1
Cre16.g676150	19861083	<i>MSD3</i>	Mn superoxide dismutase	3.3	11	24	3.5	7.4
Cre17.g712100	19866724	<i>MDAR</i>	Monodehydroascorbate reductase	31	66	140	2.1	4.4
Cre10.g456750	19872947	<i>DHAR1</i>	Dehydroascorbate reductase	8.5	24	79	2.9	9.3
Cre02.g077100	19869361	<i>GSH1</i>	Glutathione synthetase	46	70	133	1.5	2.9
Cre17.g708800	19867603	<i>GSH2</i>	Glutathione synthetase	12	9.2	7.7	0.78	0.65
Cre06.g262100	19863211	<i>GSHR1</i>	Glutathione reductase	22	27	43	1.2	1.9
Cre02.g132850	19869004	<i>GSHR2</i>	Glutathione reductase	50	45	37	0.89	0.74

SUPPLEMENTAL TABLE S4. Primers sequences used for cloning of VTC2. VTC2.D2 and VTC2.A628 primers were used to PCR amplify the VTC2 coding sequence and to insert the TEV protease cleavage site and a C-terminal His6-tag. PE-277 and PE-278 primers were used to introduce AttB1 and AttB2 recombination sites. ^aPrimer sequences are written 5' to 3'.

Name	Primer Sequence ^a
VTC2.D2.Forward	GAGAACCTGTACTTCCAGGGTGATTCTCTTCAGGCGCTGC
VTC2.A628.Reverse	ATTAGTGATGATGGTGGTGATGAGCGCTGGAGCCGAAG
PE-277.Forward	GGGGACAAGTTTGTACAAAAAAGCAGGCTCGGAGAACCCTGTACTTCCAG
PE-278. Reverse	GGGGACCACTTTGTACAAGAAAGCTGGGTATTAGTGATGATGGTGGTGATG

SUPPLEMENTAL TABLE S5. Primers sequences used for real-time PCR. ^aProtein IDs correspond to the Augustus 10.2 annotation of the version 4 assembly (FM4). ^bPrimer sequences are written 5' to 3'.

Name	Protein ID ^a	Forward Primer Sequence ^b	Reverse Primer Sequence ^b
<i>APX1</i>	Cre02.g087700	TCAAGGAGATCAAGGCCAAG	GCCGCTCAGTCCAGAGTAAC
<i>MSD3</i>	Cre16.g676150	CAGCCCCAACCAGGATAAC	ACCAGACCCACCCAGGAG
<i>MDAR1</i>	Cre17.g712100	GGTGCTGGGGAAGATGCTGT	ACGCACTGGTTCACGCTTTG
<i>DHAR1</i>	Cre10.g456750	ACGGCACAGAGGCCATCATC	CCCCTCCGTAAGCCCTCAA
<i>VTC2</i>	Cre13.g588150	GGGTTGGCTTCAAGGTGTGG	TTGTCTCTTGGCCCCGTCTC
<i>GSH1</i>	Cre02.g077100	ACCACCTGACCACCATCTTC	GTATATGAGCCCCACCCACA
<i>GSHR1</i>	Cre06.g262100	GCCATCAAGGTGGATGAGTT	ATAGTCGGGCTTGGTCAGC
<i>CBLP</i>	Cre13.g599400	GCCACACCGAGTGGGTGTCGTGCG	CCTTGCCGCCCGAGGCGCACAGCG
<i>UBQ2</i>	Cre09.g396400	GCGATTTCTCGTTGGGCAGT	TGGCCCATCCACTTGTCTT